RE-347J

A FINITE ELEMENT METHOD FOR THE PLASTIC BENDING ANALYSIS OF STRUCTURES

October 1968

Grumman

RESEARCH DEPARTMENT

GRUMMAN AIRCRAFT ENGINEERING CORPORATION

BETHPAGE NEW YORK

Grumman Research Department Report RE-347 J

A FINITE ELEMENT METHOD FOR THE PLASTIC BENDING ANALYSIS OF STRUCTURES†

by

H. Armen, Jr.
A. Pifko
H. S. Levine

Special Projects Section

October 1968

†Presented at the Air Force Second Conference on Matrix Methods in Structural Mechanics, Wright-Patterson Air Force Base, Ohio, 15-17 October 1968.

Approved by: Charles E. Mack, Jr.
Charles E. Mack, Jr.
Director of Research

ACKNOWLEDGMENT

This investigation was supported by the National Aeronautics and Space Administration, Langley Research Center, under Contract NAS 1-7315. The authors gratefully acknowledge the work of Joseph S. Miller in programming the analysis.

ABSTRACT

A finite element technique is presented for the plastic analysis of structures subjected to out-of-plane bending, alone or in combination with in-plane membrane stresses. The method makes use of a linear matrix equation of finite element analysis, formulated to include the effect of initial strains. This equation is applied to the plasticity problem by interpreting plastic strains as initial strains, the material nonlinearity being introduced through subsidiary stress-strain relations from an incremental plasticity theory. In addition, the analysis is combined with an incremental technique developed to account for the effects of geometric nonlinear behavior. Thus, the present analysis is capable of treating the combined effects of material and geometric nonlinearity. Application of the procedure is made to beam and arch structures in the presence of both types of nonlinearity, and to rectangular plates for which material nonlinearity alone is present.

TABLE OF CONTENTS

LIST OF ILLUSTRATIONS

LIST OF SYMBOLS

a	beam length; plate half-length
b	beam width; plate half-width
d_0	generalized nodal displacement
E	Young's modulus
e^e	elastic strain
e^o	initial strain
e^T	total strain
$H_{ij}^{(0)}(x), H_{ij}^{(1)}(x)$	zeroth and first order Hermitian polynomials
I	moment of inertia
$[k]$	element elastic stiffness matrix
$[k^*]$	element initial strain stiffness matrix
ℓ	beam element length
P_0	generalized nodal force
t	half thickness of beam or plate element
u,v	in-plane displacement components (plate)
U	strain energy
w	lateral displacement
w_0^*	lateral displacement at maximum elastic load
x,y	in-plane coordinates (plate)
z	lateral coordinate
$\bar{z}$	depth of elastic plastic boundary
γ^P	shearing plastic strain

ϵ	normal plastic strain
ν	Poisson's ratio
σ	normal stress
σ_{yield}	yield stress
τ	shear stress
{ }	vector quantity
[ ]	matrix quantity
'	transpose of a matrix or vector
0	subscript zero denotes nodal quantities

I. INTRODUCTION

The description of plastic behavior presents some basic difficulties to the structural analyst. These difficulties are associated with a proper description of the material phenomenon and the nonlinear nature of the resulting governing equation. Thus, the mathematical formulation of the plasticity problem makes a continuum analysis of all but the simplest structures a very formidable, if not an impossible, task. Consequently, considerable attention has been given recently to the extension of finite element techniques to include the effects of plastic behavior (Refs. 1-5). These techniques have the advantage of being capable of treating the effects of plasticity in complex structures by utilizing various algorithms for linearizing the basic nonlinear nature of the problem.

Most of the current effort concerned with the application of finite element techniques to the plasticity problem has been limited to the treatment of structures in states of membrane stress. In addition, the methods generally neglect the effects of geometric nonlinearity. These limitations are too restrictive for many important aerospace structures. Consequently, it is the purpose of the present paper to extend the methods already developed to provide for a plastic bending analysis that accounts for membrane stress states and geometric nonlinearity.

The present method makes use of a governing linear matrix equation that relates the applied loading to the nodal displacements and initial strains. For the purpose of a plasticity analysis, the plastic strains are interpreted as initial strains. Use of the initial strain concept, to treat the effects of plasticity, requires the development of appropriate matrix relations based on assumptions for the distribution of both displacement and initial (plastic) strain within a finite element. The specification of a distribution for plastic strain within a finite element forms the basis on which the present plasticity analysis depends.

Inclusion of the effects of geometric nonlinearity is primarily of concern in problems involving thin beams, plates, and shells in the plastic, as well as elastic, range. A finite element method that utilizes an incremental procedure requiring a successive modification of the element stiffness properties has been discussed in Ref. 6. This method requires the introduction of an additional stiffness matrix to account for the effects on the bending stiffness of the membrane stresses generated as a consequence of geometric nonlinearity. In addition, the effect that changes in geometry have on subsequent deformations is taken into account. This incremental procedure is incorporated into the plastic bending analysis to treat the combined effects of material and geometric nonlinearity.

II. MATERIAL NONLINEARITY-PLASTIC BENDING ANALYSIS

An important advantage of finite element techniques is the ability to specify the distribution of displacement and strain states within each finite element. This permits assumptions to be made for the distribution of plastic strain and the development of regions of plasticity within an element. These assumptions considerably reduce the complexity of the analysis by defining the distribution of plastic strain in any element, once the nodal values are determined. This feature is consistent with finite element analysis, and allows us to be concerned only with quantities at node points of the idealized structures.

For the case of membrane stress states, the plastic strains are assumed to vary in a prescribed manner in the plane of the element. For out-of-plane bending, an assumption must be made for the distribution of plastic strain through the thickness as well as in the middle surface of the element. Specifically, the present analysis assumes the plastic strains to vary linearly along the edges of a finite element between adjacent nodes, and in addition assumes a linear variation of plastic strains from the upper or lower surface of the element to an elastic-plastic boundary (or boundaries) located within the cross section of the element. These assumptions require the determination of the position of an elastic-plastic boundary based on its assumed distribution within the element during the course of loading. Thus, the present analysis utilizes the concept of a finite element in which there is a progressive development of a plastic region instead of the layered approach of Ref. 7 or the sandwich idealization of Ref. 8.

The above assumptions are made in the development of the governing linear matrix relation, which has been formulated to include the effects of initial strains. These assumptions, as applied to a typical beam finite element for which pure bending behavior has been assumed, are shown in Fig. 1. The function for the displacement in the z-direction is assumed to be of cubic order in the coordinate x, and is written in terms of the generalized nodal displacements as

$$\begin{aligned} w(x) = &\left(1 - 3\frac{x^2}{\ell^2} + 2\frac{x^3}{\ell^3}\right) w_i + \left(3\frac{x^2}{\ell^2} - 2\frac{x^3}{\ell^3}\right) w_j \\ &+ \left(x - 2\frac{x^2}{\ell} + \frac{x^3}{\ell^2}\right) w_{,x_i} + \left(\frac{x^3}{\ell^2} - \frac{x^2}{\ell}\right) w_{,x_j} \end{aligned} \tag{1}$$

In choosing a displacement function, it is important to include all fundamental strained states and all rigid body terms. Equation (1) satisfies these requirements for a beam element, and in the case of a uniform bending stiffness, EI, allows for a constant shear load and linearly varying moment along the length of the element. The plastic strain distribution is assumed to vary linearly in the x-direction from its value at the upper (or lower) surface at node i, represented in Fig. 1 as ϵ_{0i}, to its value at the upper (or lower) surface at node j, represented as ϵ_{0j}. This assumed distribution is written as

$$\epsilon = \left(\frac{z - \bar{z}}{t - \bar{z}}\right)\left[\epsilon_{0i}\left(1 - \frac{x}{\ell}\right) + \epsilon_{0j}\left(\frac{x}{\ell}\right)\right] \tag{2}$$

where $\bar{z}$ represents the depth of the elastic-plastic boundary. In addition, as seen from Eq. (2), it is assumed that at a node, the plastic strain varies linearly from its value at the upper or lower surface to zero at an elastic-plastic boundary located through the cross-section.

The depth of the elastic-plastic boundary, which propagates from the upper and lower surface, is measured from the neutral axis for pure bending, as shown in Fig. 1. In general, the depth of this boundary cannot be directly related to the load. Hence, the value of $\bar{z}$ must be determined from the total strain distribution, which is assumed to vary linearly through the thickness in accordance with Kirchoff's hypothesis. The functional form representing the distribution of the elastic-plastic boundary is assumed to be a linear function of the coordinate x and may be written as

$$\bar{z} = (\bar{z}_j - \bar{z}_i)\left(\frac{x}{\ell}\right) + \bar{z}_i \ . \tag{3}$$

where $\bar{z}_i$ and $\bar{z}_j$ represent the depth of the elastic-plastic boundary at nodes i and j, respectively. Thus, with the preceding assumptions, the elastic-plastic boundary consists of a surface in the interior of the element that extends over the entire area of the element and intersects the edges along straight lines joining nodes, as illustrated in Fig. 1. In addition, these assumptions eliminate the necessity of determining an elastic-plastic boundary on the faces of the element between nodes, but still require locating such a boundary through the thickness.

The present assumptions are further extended to include the effects of bending in combination with a membrane stress state. As seen in Fig. 2, this extension necessitates the determination of the position of the elastic-plastic boundary relative to both the upper and/or lower surface. The functional representation of the plastic strain distribution and the representation of the elastic-plastic boundary are taken similar to Eqs. (2) and (3) written for both the upper and lower surface. A second matrix, in addition to the usual stiffness matrix, termed the initial stress stiffness matrix (to be discussed in the next section), is also introduced to account for the effects of the membrane load on the bending stiffness. This problem also requires the introduction of a second displacement component, u, acting in the axial direction,

$$u(x) = \left(1 - \frac{x}{\ell}\right)u_i + \left(\frac{x}{\ell}\right)u_j \tag{4}$$

It should be noted that although the functional form of the plastic strain distribution, as shown in Fig. 2, does assume the existence of a neutral axis located within the cross section of the beam element, the present analysis is capable of considering plastic sections in which the neutral axis is not located within the thickness of the beam, i.e., the upper and lower strains are of the same sign. This situation occurs with the application, or generation, of large membrane stresses as compared to the existing bending stresses. The treatment of this situation is accomplished by modifying the functional form of the plastic strain distribution given in Fig. 2.

The present method has also been extended to treat the more complex problem of the plastic bending of a plate. A typical rectangular plate element is shown in Fig. 3. The displacement function chosen is the one originally used by Bogner, Fox, and Schmit, (Ref. 9), and is in terms of products of first order Hermitian polynomials. The components of initial strain are assumed to vary as products of zero order Hermitian polynomials in the plane of the element and linearly through the cross-section from their values at the upper (or lower) surface to zero at the elastic-plastic boundary. The depth of the boundary through the thickness, which must be determined at each of the four nodes of the rectangular element, is computed from the total strains by means of the following relation:

$$\bar{z}_{ij} = \frac{\sigma_{yield}\, t}{\sqrt{(J_{2\,max})_{ij}}} \qquad i,j = 1,2$$

where

$$(J_{2\,max})_{ij} = \frac{E}{(1+\nu)^2}\left[\left(e_x^T - e_y^T\right)^2 + e_x^T e_y^T + \frac{3}{4}\left(\gamma_{xy}^T\right)^2 + \frac{\nu}{(1-\nu)^2}\left(e_x^T - e_y^T\right)^2\right]_{ij}$$

and the superscript T denotes total strains.

The function defining the elastic-plastic boundary in the plane of the element is assumed to be in the form of products of zero order Hermitian polynomials as shown in Fig. 3. The foregoing assumptions associated with the plastic strain distribution and the representation of the elastic-plastic boundary ensure compatibility of these quantities along element boundaries.

A. Method of Analysis

Once the assumption is made on the distribution of displacement, the total strain distribution can be expressed in terms of nodal displacements by making use of the appropriate strain displacement relations in conjunction with the assumed displacement function. This relation can be written in matrix form as follows:

$$\left\{e^T\right\} = [W] \left\{d_0\right\} \tag{5}$$

where $\left\{e^T\right\}$ is the vector of total strains

$\left\{d_0\right\}$ is the vector of generalized nodal displacements.

The assumed distribution of plastic strains can be written in terms of their nodal quantities as

$$\left\{\epsilon\right\} = [W_p] \left\{\epsilon_0\right\} \tag{6}$$

where $\left\{\epsilon_0\right\}$ is the vector of nodal plastic strains.

The matrices $[W]$ and $[W_p]$ are, in general, functional matrices which depend explicitly on the assumptions made for the distribution of displacement and initial strain, respectively, within the element. Specifically, the assumptions discussed above for the beam and plate elements are used in the formation of $[W]$ and $[W_p]$ in the present analysis. The element stiffness properties in the presence of initial strains are developed on the basis of these two functional matrices. They are obtained by substituting Eqs. (5) and (6) into the expression for strain energy and then employing Castigliano's first theorem. To this end, the expression for strain energy, excluding terms that are independent of displacements, which explicitly contains the effect of initial strains may be written as

$$U = \frac{1}{2} \iiint_V \left\{e^T\right\}' [E] \left\{e^T\right\} dV - \iiint_V \left\{e^T\right\}' [E] \left\{\epsilon\right\} dV \tag{7}$$

where the elements of the matrix $[E]$ are the coefficients associated with the appropriate linear stress strain relations. Substitution of Eq. (5) and the assumed plastic strain distribution of Eq. (6) into Eq. (7) leads to

$$U = \frac{1}{2} \left\{d_0\right\}' [k] \left\{d_0\right\} - \left\{d_0\right\}' [k^*] \left\{\epsilon_0\right\} \tag{8}$$

where

$$[k] = \iiint_V [W]' [E][W] dV \tag{9}$$

$$[k^*] = \iiint_{V_p} [W]' [E][W_p] dV \tag{10}$$

The matrix $[k]$ represents the element elastic stiffness matrix and depends only on the assumption made for element displacements. The second integral, Eq. (10), represents the initial strain stiffness matrix which is dependent on the assumptions for both total and plastic strains. The quantity V_p in Eq. (10) is the volume of the plastic region in each element as determined by the representation of the elastic-plastic boundary. Consequently, the elements of the initial strain stiffness matrix $[k^*]$ will be a function of, among other quantities, the depth of the elastic-plastic boundary at each node, and must therefore be continuously computed during the course of loading. The initial strain matrix for the beam element subjected to pure bending and that for combined bending and axial load are given in Appendix A and the initial strain matrix associated with the rectangular plate bending element is presented in Appendix B.

Application of Castigliano's theorem to Eq. (7) yields the governing linear matrix equation for an individual finite element

$$\frac{dU}{d\{d_0\}} = \left\{P_0\right\} = [k] \left\{d_0\right\} - [k^*] \left\{\epsilon_0\right\} \tag{11}$$

where $\left\{P_0\right\}$ is the vector of generalized nodal forces.

A similar equation is also developed in incremental form in anticipation of combining plasticity with the incremental geometric nonlinear analysis. This equation is written as follows:

$$\left\{\Delta P_0\right\} = [k] \left\{\Delta d_0\right\} - [\bar{k}] \left\{\Delta \epsilon_0\right\} \tag{12}$$

It should be emphasized that the initial strain stiffness matrix associated with the increment of plastic strain $\left\{\Delta \epsilon_0\right\}$ in Eq. (12) is written as $[\bar{k}]$ to distinguish it from the initial strain stiffness matrix $[k^*]$ associated with the total plastic strain $\left\{\epsilon_0\right\}$. These matrices may differ substantially, since the functional form assumed for the distribution of total plastic strain will not, in general, coincide with the assumed distribution associated with the increment of plastic strain. In the present analysis, ϵ_0 was assumed to vary linearly through the thickness from the upper and/or lower surface to the elastic-plastic boundary. This assumption implies a bilinear distribution of $\Delta \epsilon_0$. The specification of a distribution of this form requires the determination of a value of the plastic strain increment at some intermediate point in the cross section, in addition to a value at the upper and/or lower surface.

To avoid the added complexities associated with the use of Eq. (12), we may alternatively use an incremental form of Eq. (11) as follows:

$$\left\{\Delta P_0\right\}^i = [k] \left\{\Delta d_0\right\}^i - \left\{\Delta q\right\}^i \tag{13}$$

where

$$\left\{\Delta q\right\}^i = \Delta \left([k^*]^i \left\{\epsilon_0\right\}^i \right) = [k^*]^i \left\{\epsilon_0\right\}^i - [k^*]^{i-1} \left\{\epsilon_0\right\}^{i-1}$$

and the superscripts i and $i-1$ refer to the current and preceding loading step, respectively. In Eq. (13), the product of the initial strain stiffness matrix and the total plastic strain is considered as a vector of fictitious loads. The increments of these fictitious loads, represented as $\left\{\Delta q\right\}$, are determined at any step by subtracting their current values from those computed in the preceding step. In this manner, only total values of plastic strain are utilized in the governing linear matrix equation. The desired form of the equation is obtained by grouping the increments of generalized nodal forces and fictitious forces, resulting in the following equation:

$$[k] \left\{\Delta d_0\right\}^i = \left\{\Delta P_0\right\}^i + \left\{\Delta q\right\}^{i-1} \tag{14}$$

Here, it is seen that the values of the increments of fictitious loads introduced into Eq. (14) are values taken to be equal to those computed in the preceding load increment. The use of this type of predictor procedure is necessary because the depth of the elastic-plastic boundary (and the current value of plastic strain) at those nodes of the structure in the plastic range can be determined, in general, only from the stress (or strain) distribution computed at the end of the load step. The position of the elastic-plastic boundary is determined at the end of each load increment, and is assumed to remain fixed during the next increment.

Equation (14) is written for each element in the structural idealization and then appropriately assembled to form the over-all linear matrix equation for the entire structure. This equation, not shown here, is identical in form to Eq. (14). The incremental solution technique using this equation reduces to a sequence of linear problems in which the applied loading is constantly modified by the fictitious force vector.

B. Plasticity Relations

The foregoing matrix equations must be used in conjunction with an appropriate plasticity theory. Plasticity is introduced into Eq. (14) through subsidiary stress-strain relations provided by this theory. In the present paper, consideration is given to both elastic, strain-hardening or ideally plastic material behavior. For both types of behavior, the total strain increment at a node can be written as the sum of an elastic and plastic component, represented as $\left\{\Delta e_0^e\right\}$ and $\left\{\Delta \epsilon_0\right\}$, respectively, in the following equation:

$$\left\{\Delta e_0^T\right\} = \left\{\Delta e_0^e\right\} + \left\{\Delta \epsilon_0\right\} \tag{15}$$

In addition, the increment of elastic strain is related to the stress increment, $\left\{\Delta\sigma\right\}$, by means of Hooke's Law. Thus, Eq. (15) can be written as

$$\left\{\Delta e^T\right\} = [E]^{-1} \left\{\Delta\sigma\right\} + \left\{\Delta\epsilon\right\} \tag{16}$$

For an elastic, strain-hardening material, we make use of a linear incremental relation between plastic strain and stress

$$\left\{\Delta\epsilon\right\} = [C] \left\{\Delta\sigma\right\} \tag{17}$$

This relationship is represented in a general form by the matrix $[C]$ in Eq. (17). The formulation of this matrix is directly related to the plasticity theory chosen for use, i.e., these elements may be determined by using an isotropic hardening theory or the kinematic hardening theory of plasticity. The elements of this array for plane stress, obtained by using Drucker's postulate with the Prager-Ziegler kinematic hardening theory, are explicitly given in Ref. 1.

Substituting Eq. (17) into Eq. (16) leads to an incremental stress-strain relation given in the following equation:

$$\left\{\Delta\sigma\right\} = [R]^{-1} \left\{\Delta e^T\right\} \tag{18}$$

where

$$[R] \equiv [E]^{-1} + [C]$$

It should be noted that there is no unique stress increment for a given plastic strain increment vector. Therefore, the matrix [C], given in Ref. 1, is singular. However, the matrix [R], defined in Eq. (18), will possess an inverse, thereby providing the necessary coefficients relating the stress increment to the increment of total strain.

The increments in total strain at a node, $\left\{\Delta e_0^T\right\}$, are obtained from the increments of displacement by using Eq. (5) in incremental form as follows:

$$\left\{\Delta e_0^T\right\} = [W_0] \left\{\Delta d_0\right\} \tag{19}$$

where $[W_0]$ is defined at a node. It should be noted from the above equation and Eq. (5) that the functional form chosen to represent the increments of total strain, $\left\{\Delta e_0^T\right\}$, is identical to that used in the representation of their full values, $\left\{e_0^T\right\}$. Thus, having obtained the increments of displacement from the solution of the total linear matrix equation in the form of Eq. (14), Eqs. (15-19) represent the necessary relations that must be used to obtain the complete solution for increments of stress and strain, assuming elastic strain-hardening material behavior. After summing all incremental quantities, new values of the increments of fictitious load, $\left\{\Delta q\right\}$, are determined for each element in the plastic range and the procedure is repeated until the desired maximum values of the loads are reached.

Consideration of elastic, ideally plastic material behavior is necessary for predicting the collapse load of a given structure in a given loading situation. The two conditions to be satisfied for multiaxial elastic, ideally plastic material behavior are;

1) the stress increment vector must remain tangent to the loading surface, and
2) the plastic strain increment vector must remain normal to the loading surface, where the loading function is the representation, in stress space, of the initial yield function, or the subsequent yield function after some plastic deformation has occurred.

The above conditions are expressed analytically for the case of plane stress and using the von Mises yield condition by the following two equations:

$$(\sigma_x - \tfrac{1}{2}\sigma_y)d\sigma_x + (\sigma_y - \tfrac{1}{2}\sigma_x)d\sigma_y + 3\tau_{xy}d\tau_{xy} = 0 \tag{20}$$

$$\frac{d\epsilon_x}{(\sigma_x - \frac{1}{2}\sigma_y)} = \frac{d\epsilon_y}{(\sigma_y - \frac{1}{2}\sigma_x)} = \frac{d\gamma^p_{xy}}{3\tau_{xy}} = d\lambda \tag{21}$$

where $d\lambda$ is a positive scalar quantity.

If we consider the differential of the stress components as incremental quantities, the implicit differential of Eq. (20) provides a linear relation among the components of stress increment, represented in matrix form as follows:

$$\{\Delta\sigma\} = [\bar{E}]\{\Delta\sigma\} \tag{22}$$

Expressing $\Delta\sigma_x$ in terms of $\Delta\sigma_y$ and $\Delta\tau_{xy}$ yields the elements of the matrix $[\bar{E}]$ as

$$[\bar{E}] = \begin{bmatrix} 0 & -M_1 & -M_2 \\ 0 & 1 & 0 \\ 0 & 0 & 1 \end{bmatrix}$$

where

$$M_1 = (\sigma_y - \tfrac{1}{2}\sigma_x)/(\sigma_x - \tfrac{1}{2}\sigma_y)$$

$$M_2 = 3\tau_{xy}/(\sigma_x - \tfrac{1}{2}\sigma_y)$$

If we replace $d\epsilon_{ij}$ by $\Delta\epsilon_{ij}$, Eq. (17) provides a linear relation between components of plastic strain increment, written as

$$\left\{\Delta\epsilon\right\} = [\tilde{E}] \left\{\Delta\epsilon\right\} \tag{23}$$

Then, expressing $\Delta\epsilon_y$ and $\Delta\gamma_{xy}$ in terms of $\Delta\epsilon_x$ gives the elements of the matrix $[\tilde{E}]$

$$[\tilde{E}] = \begin{bmatrix} 1 & 0 & 0 \\ M_1 & 0 & 0 \\ M_2 & 0 & 0 \end{bmatrix}$$

It is apparent from Eq. (20) and (21) that only two of the three components of stress increment and only one of the three components of plastic strain increment are required to obtain the remaining components. Thus, only three of the six quantities are independent variables. The increments of stress and plastic strain can now be written in terms of a vector, $\left\{\Delta\omega\right\}$, representing these independent quantities, arbitrarily chosen as $\Delta\epsilon_x$, $\Delta\sigma_y$, and $\Delta\tau_{xy}$,

$$\left\{\Delta\omega\right\} = \begin{Bmatrix} \Delta\epsilon_x \\ \Delta\sigma_y \\ \Delta\tau_{xy} \end{Bmatrix} \tag{24}$$

Equations (22) and (23) may now be rewritten to relate the increments of stress and plastic strain in terms of $\{\Delta\omega\}$

$$\{\Delta\sigma\} = [\bar{E}]\ \{\Delta\omega\} \tag{25}$$

and

$$\{\Delta\epsilon\} = [\tilde{E}]\ \{\Delta\omega\} \tag{26}$$

A relation between the vector $\{\Delta\omega\}$ and the increment of total strain is obtained by substituting Eqs. (25) and (26) into Eq. (16)

$$\{\Delta e^T\} = [E^*]\ \{\Delta\omega\} \tag{27}$$

where

$$[E^*] \equiv [E]^{-1}\ [\bar{E}] + [\tilde{E}]$$

Once again, as in the case of strain hardening behavior, increments of displacement and total strain are obtained from the linear matrix equations. The solution for $\{\Delta\omega\}$ from Eq. (27) and its substitution into Eqs. (25) and (26) represent the procedure necessary to obtain the complete solution for displacements, stresses, and strains for any increment, assuming elastic-ideally plastic material behavior.

III. MATERIAL AND GEOMETRIC NONLINEARITY

For the preceding theory and applications, it is assumed that the strain-displacement relations are linear although the stress-strain law is not. The implementation of a nonlinear stress-strain relation for the characterization of material behavior merely depends on the absolute magnitudes of the elongations and shears existing in a body. When they exceed a certain value, nonlinear material characteristics become important and must be included to gain an insight into the response of the structure to further loading. Although the magnitudes of the shears and elongations may be sufficiently large to necessitate the inclusion of plastic effects, their values and the value of the angles of rotation may still be small compared to unity. If this condition, and the additional condition that the squares and products of angles of rotation may be neglected as compared to the elongations and shears, remain valid, then the use of linear strain-displacement relations is justified. Thus, material nonlinearity can exist independently of geometric nonlinearity.

For flexible bodies (beams, plates, shells), the second condition (that on the squares and products of rotation) is not satisfied in many instances. Under these circumstances it is unjustifiable to neglect the terms containing the squares and products of the rotations in the strain-displacement relations. Furthermore, the linear equilibrium equations are no longer valid and nonlinear terms consistent with the inclusion of rotations in the strain-displacement relations should be retained. Thus, stresses that multiply rotations should not automatically be dropped in deference to those that appear linearly in the equilibrium equations.

Geometric nonlinearity can exit independently of physical nonlinearity since small shears and elongations do not imply small angles of rotation. Problems requiring the consideration of geometric nonlinearity alone include the question of stability of elastic equilibrium, the deformation of bodies having initial stresses, large deflection of beams, plates and shells, and torsion and bending in the presence of axial forces. For these situations, the effect of geometric nonlinearity must be taken into account not only in the strain displacement relations, but in determining changes in the length of line elements, and in formulating the conditions of equilibrium of the volume element. In addition, if the magnitudes of the strains become too large, it then becomes necessary to include material nonlinearity through the stress-strain relations.

In the following, the procedure developed for material nonlinearity is expanded to include geometric nonlinearity. Although only elastic perfectly-plastic results are given, the method is equally applicable and easily adaptable to strain-hardening behavior using the procedure outlined in the previous section. Representative structures chosen to illustrate the significant features of combined geometric and material nonlinearity are the restrained beam and the circular arch.

Martin (Ref. 6) has presented an incremental numerical method, based on the direct stiffness approach, which is generally applicable for the treatment of problems involving geometric nonlinearity. This procedure approximates the nonlinear behavior by a sequence of linear steps. Either loading or displacement may be applied incrementally. This procedure also requires the introduction of an initial stress stiffness matrix, in addition to the conventional stiffness matrix, to account for the effects on the bending stiffness of membrane loads, i.e., the effects of rotations on strains. Thus, the implementation of this matrix in addition to the initial strain matrix represents the required modifications for the development of an incremental procedure to account for both types of nonlinearity.

A general development of the matrices discussed above and the method of solution to the problem of combined nonlinearity is obtained by following the procedure outlined in Ref. 6 with modifications associated with the inclusion of plasticity. The total elastic strain may be written as the sum of three components, i.e.,

$$\left\{e^{e}\right\} = \left\{e^{o}\right\} + \underbrace{\left\{\Delta e^{T}\right\} - \left\{\Delta \epsilon\right\}}_{\left\{\Delta e^{e}\right\}} \tag{28}$$

where $\left\{e^{o}\right\}$ is the initial elastic strain vector (equal to P_0/AE for the beam column, and related to the initial stresses σ_x^o, σ_y^o, τ_{xy}^o for the two dimensional plate problem). The vector $\left\{\Delta e^{T}\right\}$ is the additional total strain developed within the increment of load. This strain increment is related to the increments of displacement through the strain-displacement relations which must now include the nonlinear rotation terms. For a beam column element, this relationship is given by

$$\Delta e^{T} = \frac{d(\Delta u)}{dx} + \frac{1}{2}\left(\frac{d(\Delta w)}{dx}\right)^{2} - z\,\frac{d^{2}(\Delta w)}{dx^{2}} \tag{29}$$

where Δu and Δw represent the increments in the axial and lateral displacements of the middle surface of the beam. The usual Bernoulli-Euler kinematic beam theory assumptions were made to obtain Eq. (29). The first term in the above equation represents the extension of the centerline of the beam, the second term is the contribution to the extensional strain due to lateral deflection (the rotation term), and the last term is the conventional bending strain term arising from the condition that normals to the neutral axis should, after deformation, remain straight and normal to the center-line and unextended. The corresponding strain-displacement relations for a plate are

$$\begin{aligned}
\Delta e_x^T &= \frac{\partial(\Delta u)}{\partial x} + \frac{1}{2}\left(\frac{\partial(\Delta w)}{\partial x}\right)^2 - z\,\frac{\partial^2(\Delta w)}{\partial x^2} \\
\Delta e_y^T &= \frac{\partial(\Delta v)}{\partial y} + \frac{1}{2}\left(\frac{\partial(\Delta w)}{\partial y}\right)^2 - z\,\frac{\partial^2(\Delta w)}{\partial y^2} \\
\Delta \gamma_{xy}^T &= \frac{\partial(\Delta u)}{\partial y} + \frac{\partial(\Delta v)}{\partial x} + \frac{\partial(\Delta w)}{\partial x}\,\frac{\partial(\Delta w)}{\partial y} - 2z\,\frac{\partial^2(\Delta w)}{\partial x \partial y}
\end{aligned} \tag{30}$$

The functional form for the increments in displacement for the beam column is chosen to be identical to that given in Eqs. (1,4) for the total displacement, i.e.,

$$\begin{aligned}
\Delta w(x) &= \sum_{i=1}^{2} \left[H_{0i}^{(1)}(x)\Delta w_i + H_{1i}^{(1)}(x)\Delta w,_{x_i} \right] \\
\Delta u(x) &= \sum_{i=1}^{2} H_{0i}^{(0)}(x)\Delta u_i
\end{aligned} \tag{31}$$

where the definitions of the Hermitian polynomials may be obtained by comparing corresponding terms in Eqs. (1), (4), and (31). A representation identical to that giver in Ref. 9

may be used for the increment of lateral displacement for the plate element. The incremental relationship between total strain and generalized nodal displacements is obtained by taking appropriate derivatives of the assumed displacement functions.

The increment in elastic strain energy from an initial elastic strain state, $\left\{e^{o}\right\}$, may be written as

$$\Delta U = \iiint_V \left[\int_{\{e^{o}\}}^{\{e^{o}\}+\{\Delta e^{e}\}} \left\{\sigma\right\}' \left\{de^{e}\right\} \right] dV \tag{32}$$

Integrating the above equation between the prescribed limits of strain and using the following relations:

$$\left\{\sigma\right\} = [E] \left\{e^{e}\right\}$$

$$\left\{\sigma^{o}\right\} = [E] \left\{e^{o}\right\}$$

and

$$\left\{\Delta e^{e}\right\} = \left\{\Delta e^{T}\right\} - \left\{\Delta\epsilon\right\} ,$$

we can write the increment of strain energy as

$$\Delta U = \frac{1}{2} \iiint_V \left\{\Delta e^{T}\right\}' [E] \left\{\Delta e^{T}\right\} dV - \iiint_V \left\{\Delta e^{T}\right\}' [E] \left\{\Delta\epsilon\right\} dV$$

$$+ \iiint_V \left\{\sigma^{o}\right\}' \left\{\Delta e^{T}\right\} dV + \frac{1}{2} \iiint_V \left\{\Delta\epsilon\right\}' [E] \left\{\Delta\epsilon\right\} dV - \iiint_V \left\{\sigma^{o}\right\}' \left\{\Delta\epsilon\right\} dV \tag{33}$$

Only those terms in the above equation that contain $\left\{\Delta e^T\right\}$, which is a function of the increment of nodal displacement, will contribute to the incremental load-deflection-initial strain relationship. The remaining terms are arbitrary constants. Upon neglecting higher order terms in the increments of displacement, the first term in Eq. (33) leads to the conventional stiffness matrix. The second term yields the initial strain matrix, and the third term leads to the initial stress stiffness matrix. In the development of the latter matrix the work done by the in-plane stresses and the generation of additional membrane stresses, resulting from the effects of geometric nonlinearity, are both taken to be zero during the application of an increment of lateral load. These considerations constitute the linearization of the procedure during an increment of load.

Consistent with the incremental procedure of the previous section, the increment of plastic strain may be written as

$$\Delta\epsilon^{i} = \epsilon^{i} - \epsilon^{i-1}$$

Substituting the above equation into Eq. (33) and then making use of Castigliano's theorem leads to the following relation for an individual element:

$$\left\{\Delta P_0\right\}^i = [k^{(0)}]\left\{\Delta d_0\right\}^i + [k^{(1)}]\left\{\Delta d_0\right\}^i - \left[[k^*]^i\left\{\epsilon_0\right\}^i - [k^*]^{i-1}\left\{\epsilon_0\right\}^{i-1}\right] \tag{34}$$

where

$$[k^{(0)}] = \iiint_V [W]'[E][W]dV ,$$

the conventional stiffness matrix,

$$[k^{(1)}] = \iiint_V [\tilde{W}]'[\sigma_0][\tilde{W}]dV ,$$

the initial stress stiffness matrix, and

$$[k^*] = \iiint_{V_p} [W]'[E][W_p]dV ,$$

the initial strain stiffness matrix. The matrix $[\tilde{W}]$ relates the increment of rotation to the increment of generalized nodal displacement and therefore represents the nonlinear contribution to the strain-displacement relations. The matrices $[W]$ and $[W_p]$ are the same as those used in the previous section.

A predictor-procedure must once again be used to obtain a solution because the location of the elastic-plastic boundary is not known a priori. Thus, the governing linear matrix equation is written in the following form:

$$\left([k^{(0)}] + [k^{(1)}] \right) \left\{ \Delta d_0 \right\}^i = \left\{ \Delta P_0 \right\}^i + \left\{ \Delta q \right\}^{i-1} \tag{35}$$

where $\{\Delta q\}$ is defined in Eq. (13), and must once again be retarded by one step in the solution procedure. Equation (35) is very nearly the same as Eq. (13) used in the previous section for the plastic bending analysis. However, because of the presence of geometric nonlinearity, the entire element stiffness matrix $[k] = [k^{(0)}] + [k^{(1)}]$ must be reformed at every step using current stress levels and geometry.

Thus, the solution procedure requires that for a generic step $[k^{(0)}]$ and $[k^{(1)}]$ are calculated by making use of the geometry and initial forces existing at the start of the step. The increment in the fictitious force, $\{\Delta q\}$, is calculated using current and immediately preceding values of the location of the elastic-plastic boundary. An increment of load is then applied, and the corresponding displacement increments calculated from the total matrix equation obtained by assembling Eq. (35) for each element. New internal forces are calculated and total stresses, strains, and displacements are obtained by summing incremental values. The new location of the elastic-plastic boundary is determined from the total strain (or stress) distribution and the process is repeated until the maximum specified load level is reached or the structure fails.

IV. RESULTS

As a demonstration of the feasibility of the plastic bending analysis, application of the method has been made to some elementary, but representative sample structures. For two of these structures (a simply supported and a cantilevered beam), results from an exact solution to the governing differential equation, assuming elastic-ideally plastic material behavior, are available for comparison. As a consequence of assuming elastic-ideally plastic behavior, and since both of the structures are statically determinate, an analytic expression can be written which relates the depth of the elastic-plastic boundary to the applied load. The finite element analysis is initially applied to the beam structures using this relationship, thus providing a means of determining the validity of assumptions made in choosing such quantities as the displacement function, the plastic strain distribution, and the representation of the elastic-plastic boundary.

Figure 4a represents a nondimensionalized load versus central deflection curve for a uniformly loaded, simply supported beam. Six elements are used in the idealization of one-half of the beam. In this figure, w_0 is the center deflection, w_0^* is the center deflection at the maximum load for which the beam is entirely elastic, and ρ represents the nondimensional load parameter,

$$\rho = \frac{p}{p_0}\left(\frac{a}{t}\right)^2 .$$

Here, p is the applied load intensity, and $p_0 = 4b \times \sigma_{yield}$. The results obtained from the finite element analysis compare quite favorably with corresponding results from the exact solution (Ref. 10), as shown in Fig. 4a. The collapse load, as determined from the near vertical slope of the load-deflection curve, is approximately 3 percent higher than the exact collapse load which occurs at a value of $\rho = 1$.

The progression of the elastic-plastic boundary through the thickness and in the plane of the element is shown in Fig. 4b. From this figure it is seen that, although the depth of the boundary at plastic nodes is exact, the assumption associated with its distribution in the plane (i.e., linearly varying to adjacent nodes), may lead to discontinuities in its representation as evidenced in the figure for load values of $\rho = 1.00$ and $\rho = 1.03$. The appearance of these discontinuities indicates that the actual boundary lies between the nodes, on the upper and lower surface of the beam. The error introduced by the assumption of a linearly varying boundary in the plane can be reduced by increasing the number of elements used in the idealization of the beam. Also to be noted in Fig. 4b is the development of a fully plastic cross section located at the center of the beam at a load of $\rho = 1$. In a continuum analysis, the development of this fully plastic cross section is sufficient to cause collapse of this structure. However, in the finite element analysis, collapse is not indicated until both cross sections of the element containing the center of the beam become fully plastic.

Results in the form of a nondimensionalized load versus tip-deflection curve for a uniformly loaded, cantilevered beam, are shown in Fig. 5a. Elastic-ideally plastic material behavior was assumed. A comparison with results from an exact solution, shown as the solid curve in the figure, indicates good correlation up to the collapse load. For this problem, as for the simply supported beam, the depth of the elastic-plastic boundary can be directly related to the applied load. This relationship was used, once again, to obtain the results shown in the figure.

The progression of the elastic-plastic boundary, through the cross section and in the plane of the elements, is shown in Fig. 5b. As indicated in the figure, the development of the boundary is much more localized for this structure than it was for the simply supported beam. Consistent with a continuum approach, collapse of this structure was indicated in the finite element analysis by the development of one fully plastic cross section at the root of the cantilever.

For both the simply supported beam and the cantilevered beam, as previously mentioned, an exact relationship between the depth of the elastic-plastic boundary at nodes in the plastic range and the applied load was used to obtain results using the finite element analysis. The justification for using this relationship, which admittedly does not exist for most structures of interest, was to check the validity of assumptions made in choosing such quantities as the displacement function, the plastic strain distribution, and the representation of the elastic-plastic boundary. As indicated by the previous results, the use of these assumptions for the finite element analysis appears to be justified.

Since, in general, the depth of the elastic-plastic boundary is not known at the current load step, results for the cantilevered beam were recomputed and a load-deflection curve, obtained by using an approximate value for the depth of the elastic-plastic boundary, is shown in Fig. 6. The value of the depth of the boundary used for any increment of load is based on the total strain distribution determined at the end of the previous load increment. The use of this procedure cannot lead to the development of a fully plastic cross section. Consequently, it is assumed that a fully plastic cross section exists at a node when plasticity has developed through a specified proportion of the thickness. The deflections and the slope of the load-deflection curve for this structure, increase quite rapidly beyond a value of load for which plasticity has developed through 80 percent of the end cross section. Thus, in the analysis this value was chosen as the criterion to determine the development of a fully plastic cross section. The degree of approximation obtained by using previous values of the depth of the boundary, when compared with the exact solution, is illustrated in the figure. As can be seen, the results compare favorably for most of the load range considered. The maximum divergence occurs in the vicinity of the collapse load and is about 7 percent.

Results are also shown in Fig. 6 for the cantilevered beam for the case of strain hardening material behavior. These results, shown as the dotted curve, are compared with the corresponding results obtained using elastic-ideally plastic behavior. The closeness of results for strain hardening and perfectly plastic behavior can be attributed to the use of Ramberg-Osgood strain hardening parameters chosen to approximate the elastic-ideally plastic stress-strain curve.

The slope of the load-deflection curve for strain hardening behavior illustrates that the beam still possesses some stiffness beyond the theoretical collapse load predicted by assuming perfectly plastic behavior.

Figure 7 illustrates the application of the procedure to a simply supported beam subjected to combined bending and axial loads. As previously discussed in Section III, the analysis for this problem requires the introduction of an initial stress stiffness matrix to account for the effects of the membrane load on the bending stiffness. The determination of the position of the elastic-plastic boundary relative to both the upper and lower surfaces is also required for this analysis. Results have been obtained for cases in which a uniform lateral load acts in conjunction with a constant tensile or compressive axial load, indicated in the figure by $T = +1000$ and $T = -1000$, respectively. These results are compared with the case of pure bending, indicated as $T = 0$. As seen in the figure, the effect of the axial compressive load is to reduce the stiffness of the structure, and the tensile load increases the stiffness, when compared to the case of pure bending. A solution to this problem by using a continuum analysis similar to the one developed for pure bending in the plastic range does not appear to be available for comparison. For the case of the compressive axial load, the lateral load was incremented to a value that resulted in the failure of the structure. This failure is indicated in Fig. 7 by the near vertical slope of the load-deflection curve. It should be noted that, for this problem, it was not necessary to develop a completely plastic cross section for collapse to occur. The reduction of the stiffness, caused by the axial compressive load and the progression of the elastic-plastic boundary through only a portion of the thickness, was sufficient to cause failure. This type of failure is associated with plastic buckling rather than the formation of a mechanism.

Application of the procedure for pure bending has been made to a simply supported, uniformly loaded, square plate. Using a 36 element idealization to represent the quarter panel, load versus central deflection curves for this structure, assuming elastic-ideally plastic and elastic-strain hardening material behavior, have been determined and are shown in Fig. 8. Once again, as in the case of the beam, the proximity of results for both types of material behavior is attributable to the choice of strain hardening parameters that approximate elastic-ideally plastic material behavior.

The collapse load for this structure, determined by assuming elastic-ideally plastic material behavior, is the value of the load at which the pattern of fully plastic elements is such that the structure becomes a mechanism. The pattern of development of the plastic region in the plane of the plate, and the progression of the elastic-plastic boundary through the thickness of the plate, is shown in Figs. 9a and 9b, respectively. In Fig. 9a the cross-hatched area represents those regions of the plate in which plasticity has developed to some degree, but extends through less than 80 percent of the cross section. The shaded area represents those regions in which plasticity extends through more than 80 percent of the thickness. A consideration of the latter region as being fully plastic leads to the development of a mechanism of collapse formed along the diagonals of the square plate, as shown in Fig. 9a. As in the case of the beam, this criterion is necessary because the determination of the depth of the elastic-plastic boundary on the basis of the total strains, cannot lead to the development of a fully plastic section.

The pattern of development of the plastic region in a narrow rectangular plate $(\eta = 0.3)$ is shown in Figs. 10a-10c, respectively. In Fig. 10a the 80 percent criterion was once again used to determine the pattern of fully plastic sections in forming the collapse mechanism. From this figure it is evident that the sections along the collapse pattern do not all lie on the diagonals of the plate.

A comparison of available upper bound solutions for the load carrying capacities of rectangular plates of various aspect ratios is shown in Fig. 11. The solid curve represents the solution (Ref. 11) obtained using the von Mises yield criterion in conjunction with assumed collapse pattern (1), shown in the figure. The dotted curve, obtained from Ref. 12, represents the upper bound solution obtained using the Tresca yield condition in conjunction with assumed collapse pattern (2). Results from the finite element analysis are represented by the solid circles. The finite element results indicate that the displacement pattern (2) provides a more accurate representation of the collapse mechanism than does pattern (1). An upper bound solution using the second displacement pattern in conjunction with the von Mises yield condition is shown as the dashed curve in Fig. 11. The results from the present analysis compare favorably with this latter solution and are slightly below it except for extremely low aspect ratios. For such narrow plates, the use of the 80 percent criterion in conjunction with the calculation of the depth of the elastic-plastic boundary from the total strain distribution of the previous step is not adequate. A relaxation of the 80 percent criterion, based on a careful examination of the load deflection history, appears to be warranted. In addition, a possible alternative might be the incorporation of an iterative procedure in the method of solution.

To illustrate the procedure associated with geometric nonlinearity and combined material and geometric nonlinearity, a simply supported, restrained beam, subjected to a uniform transverse load, is considered. Load versus central deflection curves, obtained for purely elastic and for elastic-ideally plastic material behavior, are shown in Fig. 12a. The curve for the elastic case is based both on a finite element analysis and an exact solution from Ref. 13. Load versus deflection curves, for plastic behavior, are presented for idealizations involving 6, 12, and 24 elements for one-half of the beam. Differences in the results for these idealizations only appear after the end sections at the supports become fully plastic. Beyond the value of load at which this occurs, deflections increase quite rapidly, and collapse occurs shortly thereafter with the development of another fully plastic cross section. The counterbalancing effect of geometric and material nonlinearity is vividly depicted in Fig. 12a, where it is seen that there is a region of the load-deflection curve which is very nearly linear.

Figure 12b illustrates the growth of the plastic regions of the restrained beam. The dotted line at $P = 10.74$ kips indicates a jump in the representation of the plastic region when the end section becomes fully plastic.

The load-deflection history of a circular arch subjected to a concentrated load is shown in Fig. 13. The elastic buckling load compares favorably with that obtained in Ref. 5. Load versus center deflection curves, obtained by assuming elastic-ideally plastic material behavior, are shown for two values of yield stress. The onset of collapse for this structure is appreciably hastened with the introduction of plasticity. This is attributable to the reduction of the stiffness of the structure resulting from the effects of physical nonlinearity. For this structure the effects of both types of nonlinearity are additive. As in the case of the uniformly loaded beam subjected to a constant axial compressive load, the development of a fully plastic cross section was not necessary for collapse to occur.

Figure 14 illustrates the load-deflection histories of the same arch as that used in Fig. 13, now subjected to a uniform load distribution. Once again it is seen that the effect of plasticity considerably reduces the collapse load of the structure from its elastic buckling load.

V. SUMMARY AND CONCLUSIONS

A finite element method that can account for material nonlinearity, alone, or in combination with geometrically nonlinear behavior, is presented for the out-of-plane bending analysis of structures. The initial strain concept is introduced into the finite element analysis, formulated within the framework of the direct stiffness method, to account for the effects of plasticity. These effects are introduced into the analysis by means of a fictitious load vector to be combined with the actual applied load. Thus, the method of analysis can be readily incorporated into existing finite element procedures.

Application of the method, illustrating the plastic behavior of typical structures under pure bending and bending in combination with applied axial loads, is made to simple structures and results presented. These results are compared with results from analytical solutions, where possible, for beam and plate structures. Good correlation is indicated for the load-deflection characteristics of these structures as well as for the prediction of plastic collapse loads. In addition, when compressive membrane stresses are present, the present procedure is capable of predicting failure resulting from a combination of plastic collapse and buckling. The correlation of results and the numerical stability of the procedure as applied to the sample problems substantiates the assumptions made concerning the form of the elastic-plastic boundary and the distribution of the plastic strain within each element, in addition to the use of the predictor form of the solution procedure.

Since the phenomenon of plastic deformation may lead to large displacements and rotations, the treatment of effects arising from geometric nonlinearity assumes particular significance in the solution of many important problems. Consequently, the plastic bending analysis was combined with a method capable of accounting for geometrically nonlinear behavior. This combined procedure was applied to a restrained beam and a simply supported circular arch. In the beam, the effects of geometric nonlinearity act counter to the reduction of stiffness caused by the progressive development of plasticity. Failure of this structure occurs only after the development of fully plastic cross sections. For the circular arch, the effects of both types of nonlinearity are complementary, and failure occurs as a plastic buckling phenomenon.

VI. REFERENCES

1. Isakson, G., Armen, H., Jr., and Pifko, A., "Discrete-Element Methods for the Plastic Analysis of Structures," NASA Contractors Report, CR-803, October 1967.

2. Lansing, W., Jensen, W. R., and Falby, W., "Matrix Analysis Methods for Inelastic Structures," Proc. of Conf. on Matrix Methods in Structural Mechanics, Wright-Patterson AFB, Ohio, October 26-28, 1965, AFFDL-TR-66-80.

3. Pope, G. G., "The Application of the Matrix Displacement Method in Plane Elasto-Plastic Problems," Proc. of Conf. on Matrix Methods in Structural Mechanics, Wright-Patterson AFB, Ohio, October 26-28, 1965, AFFDL-TR-66-80.

4. Marcal, P. V., "A Comparative Study of Numerical Methods of Elastic-Plastic Analysis," AIAA Journal, Vol. 6, No. 1, January 1965, p. 157.

5. Argyris, J. H., "Continua and Discontinua," Proc. of Conf. on Matrix Methods in Structural Mechanics, Wright-Patterson AFB, Ohio, October 26-28, 1965, AFFDL-TR-66-80.

6. Martin, H. C., "On the Derivation of Stiffness Matrices for the Analysis of Large Deflection and Stability Problems," Proc. of Conf. on Matrix Methods in Structural Mechanics, Wright Patterson AFB, Ohio, October 26-28, 1965, AFFDL-TR-66-80.

7. Popov, E. P., Khojesteh-Bakht, M., and Yaghmai, S., "Analysis of Elastic-Plastic Circular Plates," ASCE Journal, Engineering Mechanics Division, Vol. 93, No. EM6, pp. 49-65, December 1967.

8. Hodge, P. G., Jr., Limit Analysis of Rotationally Symmetric Plates and Shells, Chapter 3, Prentice-Hall, Inc., 1963.

9. Bogner, F. K., Fox, R. L., and Schmit, L. A., Jr., "The Generation of Inter-Element-Compatible Stiffness and Mass Matrices by the use of Interpolation Formulas," Proc. of Conf. on Matrix Methods in Structural Mechanics, Wright-Patterson AFB. Ohio, October 26-28, 1965, AFFDL-TR-66-80.

10. Prager, W. and Hodge, P. G., Jr., Theory of Perfectly Plastic Solids, Chapter 2, John Wiley & Sons, Inc., 1951.

11. Hodge, P. G., Jr., Plastic Analysis of Structures, Chapter 10, McGraw-Hill Book Co., 1959.

12. Shull, H. E. and Hu, L. W., "Load-Carrying Capacities of Simply Supported Rectangular Plates," Journal of Applied Mechanics, Vol. 30, No. 4, Trans. ASME, Series E, December 1963, p. 617.

13. Timoshenko, S. and Woinowsky-Krieger, S., Theory of Plates and Shells, Chapter 1, McGraw-Hill Book Co., 1959, p. 4.

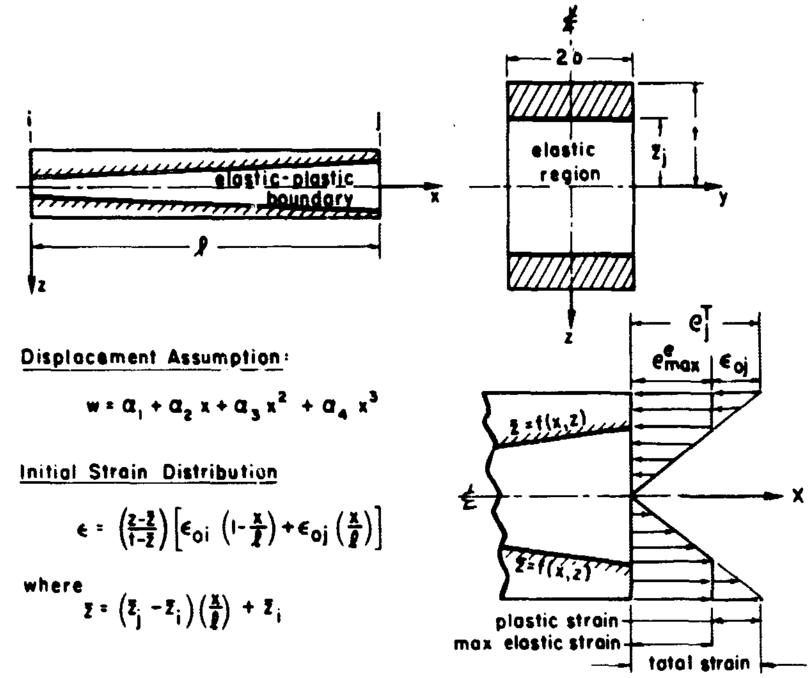

Displacement Assumption:

$$w = \alpha_1 + \alpha_2 x + \alpha_3 x^2 + \alpha_4 x^3$$

Initial Strain Distribution

$$\epsilon = \left(\frac{z-\bar{z}}{t-\bar{z}}\right)\left[\epsilon_{oi}\left(1-\frac{x}{\ell}\right)+\epsilon_{oj}\left(\frac{x}{\ell}\right)\right]$$

where

$$\bar{z} = \left(\bar{z}_j - \bar{z}_i\right)\left(\frac{x}{\ell}\right) + \bar{z}_i$$

Fig. 1 TYPICAL ELASTIC-PLASTIC BEAM ELEMENT
(PURE BENDING)

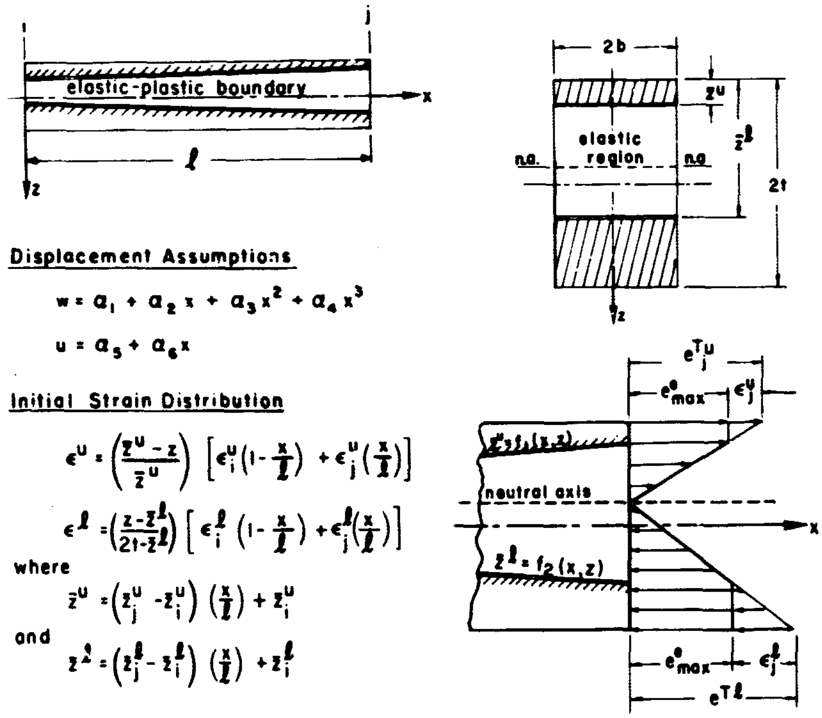

Displacement Assumptions

$$w = \alpha_1 + \alpha_2 x + \alpha_3 x^2 + \alpha_4 x^3$$

$$u = \alpha_5 + \alpha_6 x$$

Initial Strain Distribution

$$\epsilon^u = \left(\frac{\bar{z}^u - z}{\bar{z}^u}\right)\left[\epsilon_i^u\left(1-\frac{x}{\ell}\right) + \epsilon_j^u\left(\frac{x}{\ell}\right)\right]$$

$$\epsilon^\ell = \left(\frac{z-\bar{z}^\ell}{2t-\bar{z}^\ell}\right)\left[\epsilon_i^\ell\left(1-\frac{x}{\ell}\right) + \epsilon_j^\ell\left(\frac{x}{\ell}\right)\right]$$

where

$$\bar{z}^u = \left(z_j^u - z_i^u\right)\left(\frac{x}{\ell}\right) + z_i^u$$

and

$$\bar{z}^\ell = \left(z_j^\ell - z_i^\ell\right)\left(\frac{x}{\ell}\right) + z_i^\ell$$

Fig. 2 TYPICAL ELASTIC-PLASTIC BEAM ELEMENT
(BENDING AND AXIAL LOADS)

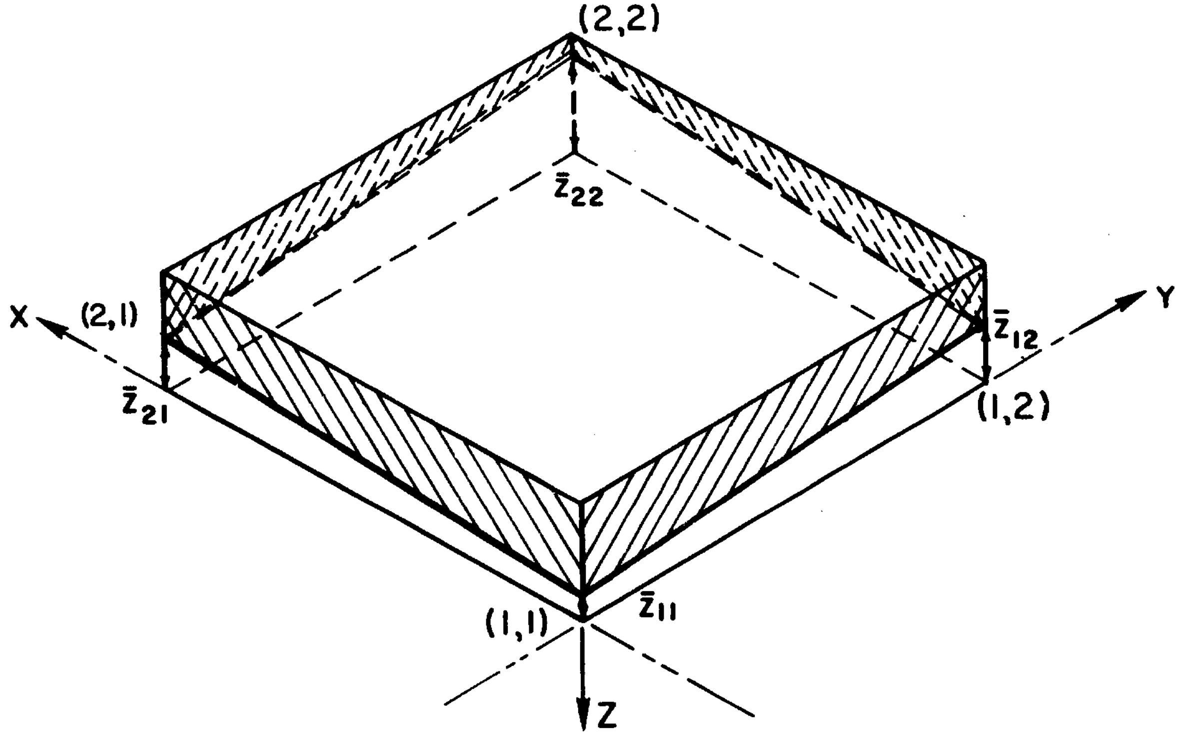

Displacement Assumption:

$$w = \sum_{i=1}^{2}\sum_{j=1}^{2}\left[H_{oi}^{(1)}(x)H_{oj}^{(1)}(y)W_{ij} + H_{1i}^{(1)}(x)\,H_{oj}^{(1)}(y)\;W,_{xij} + H_{oi}^{(1)}(x)H_{1j}^{(1)}(y)W,_{yij} + H_{1i}^{(1)}H_{1j}^{(1)}(y)W,_{xyij}\right]$$

Initial Strain Distribution:

$$\epsilon(x,y,z) = \left(\frac{z-\bar{z}}{t-\bar{z}}\right)\sum_{i=1}^{2}\sum_{j=1}^{2}H_{oi}^{(0)}(x)H_{oj}^{(0)}(y)\,\epsilon_{ij}$$

Elastic-Plastic Boundary:

$$\bar{z}(x,y) = \sum_{i=1}^{2}\sum_{j=1}^{2}H_{oi}^{(0)}(x)H_{oj}^{(0)}(y)\,\bar{z}_{ij}$$

Fig. 3 TYPICAL ELASTIC-PLASTIC RECTANGULAR PLATE ELEMENT (PURE BENDING)

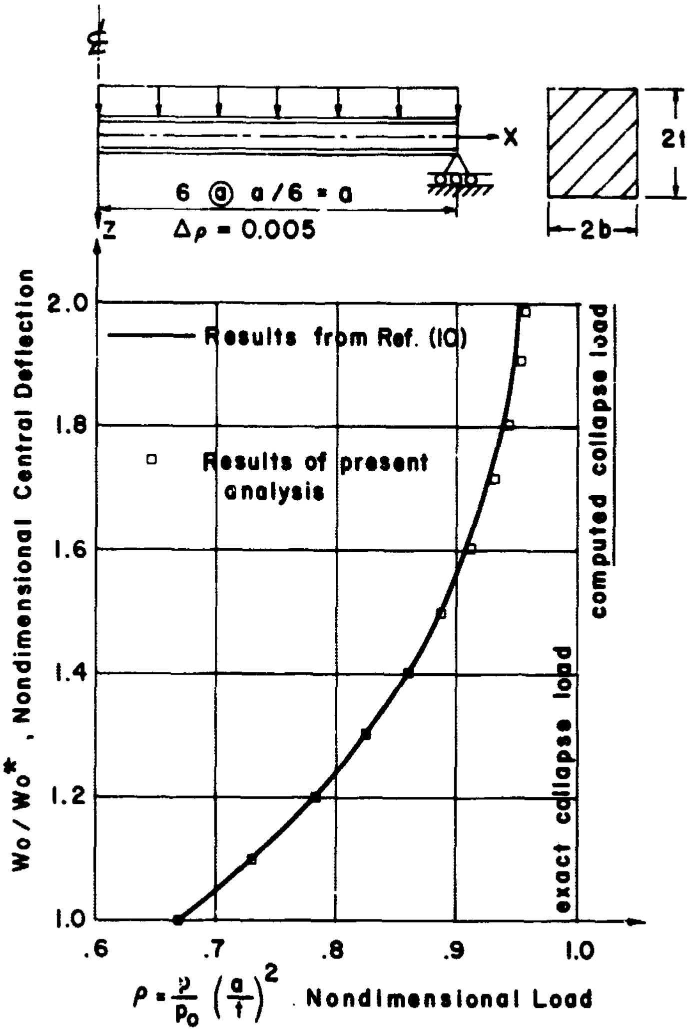

Fig. 4a LOAD VERSUS DEFLECTION OF A SIMPLY SUPPORTED BEAM

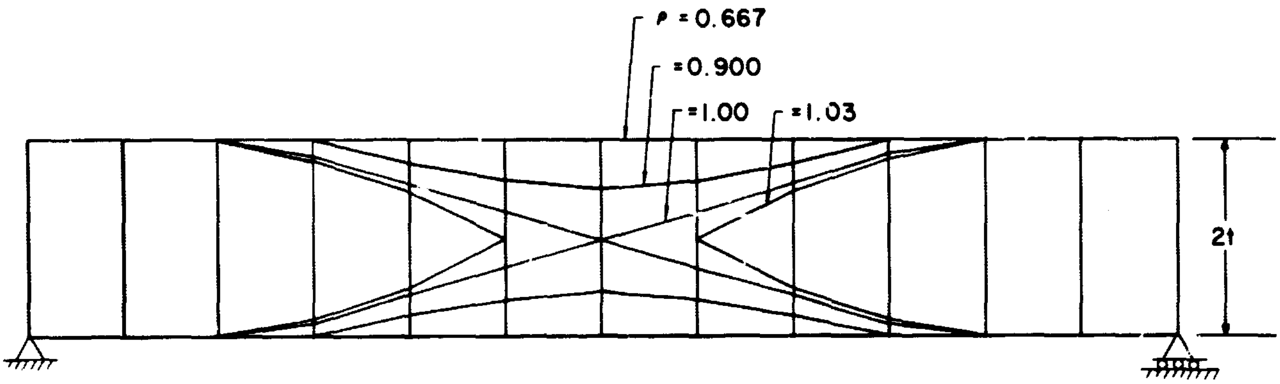

Fig. 4b PROGRESSION OF ELASTIC-PLASTIC BOUNDARY: SIMPLY SUPPORTED BEAM

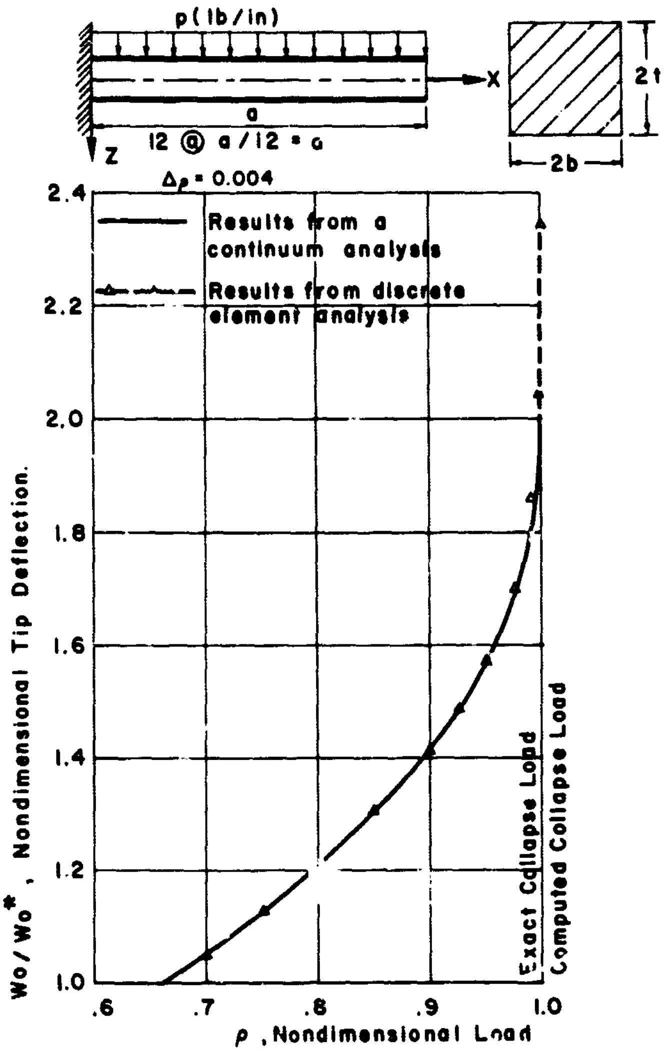

Fig. 5a LOAD VERSUS DEFLECTION OF A CANTILEVERED BEAM

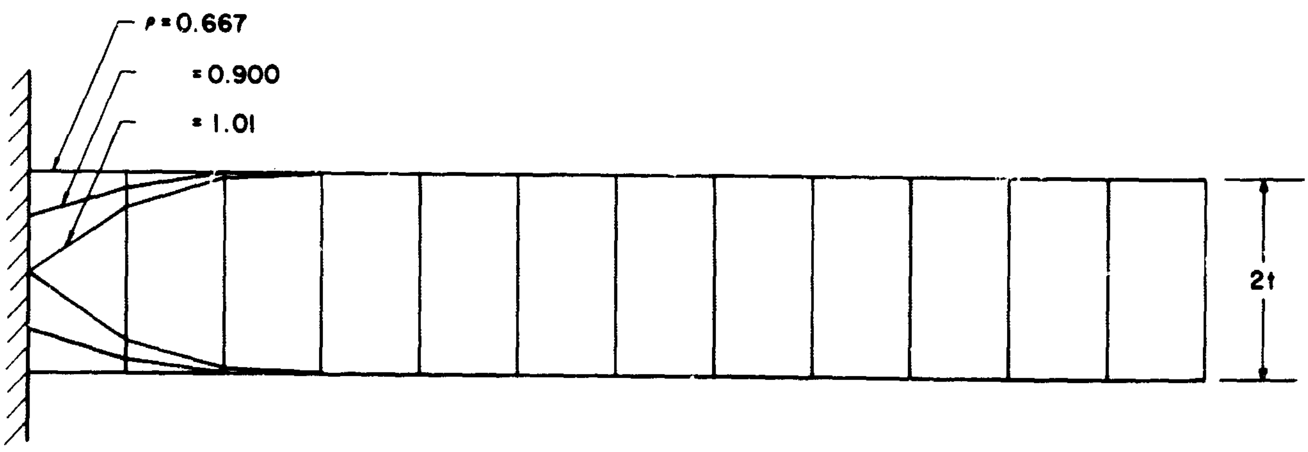

Fig. 5b PROGRESSION OF ELASTIC-PLASTIC BOUNDARY CANTILEVER BEAM

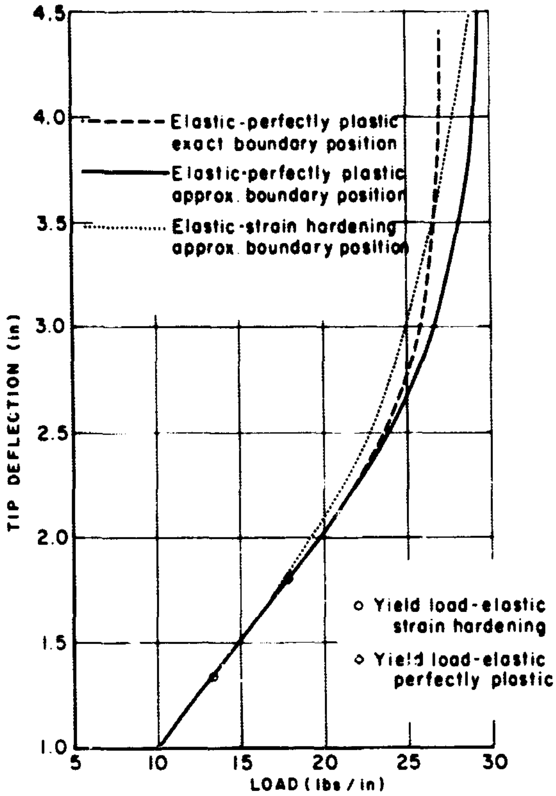

Fig.6 LOAD VERSUS TIP DEFLECTION OF CANTILEVER BEAM

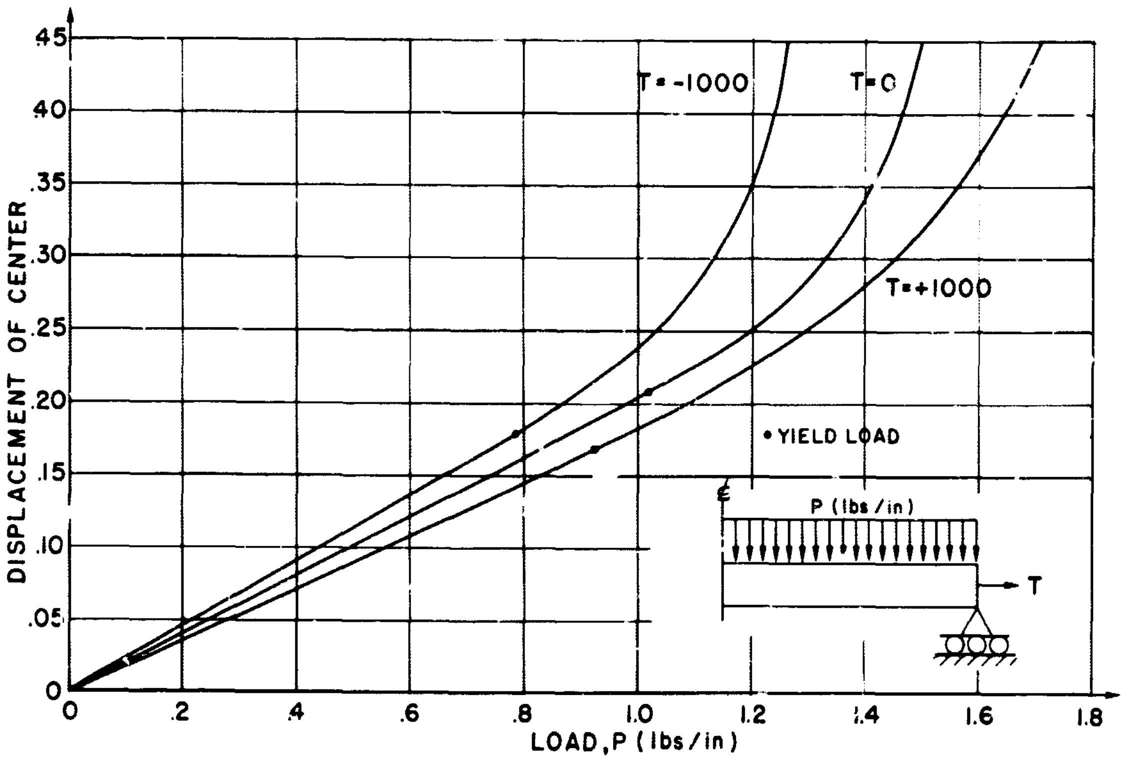

Fig.7 SIMPLY SUPPORTED BEAM SUBJECTED TO COMBINED BENDING AND AXIAL LOADS

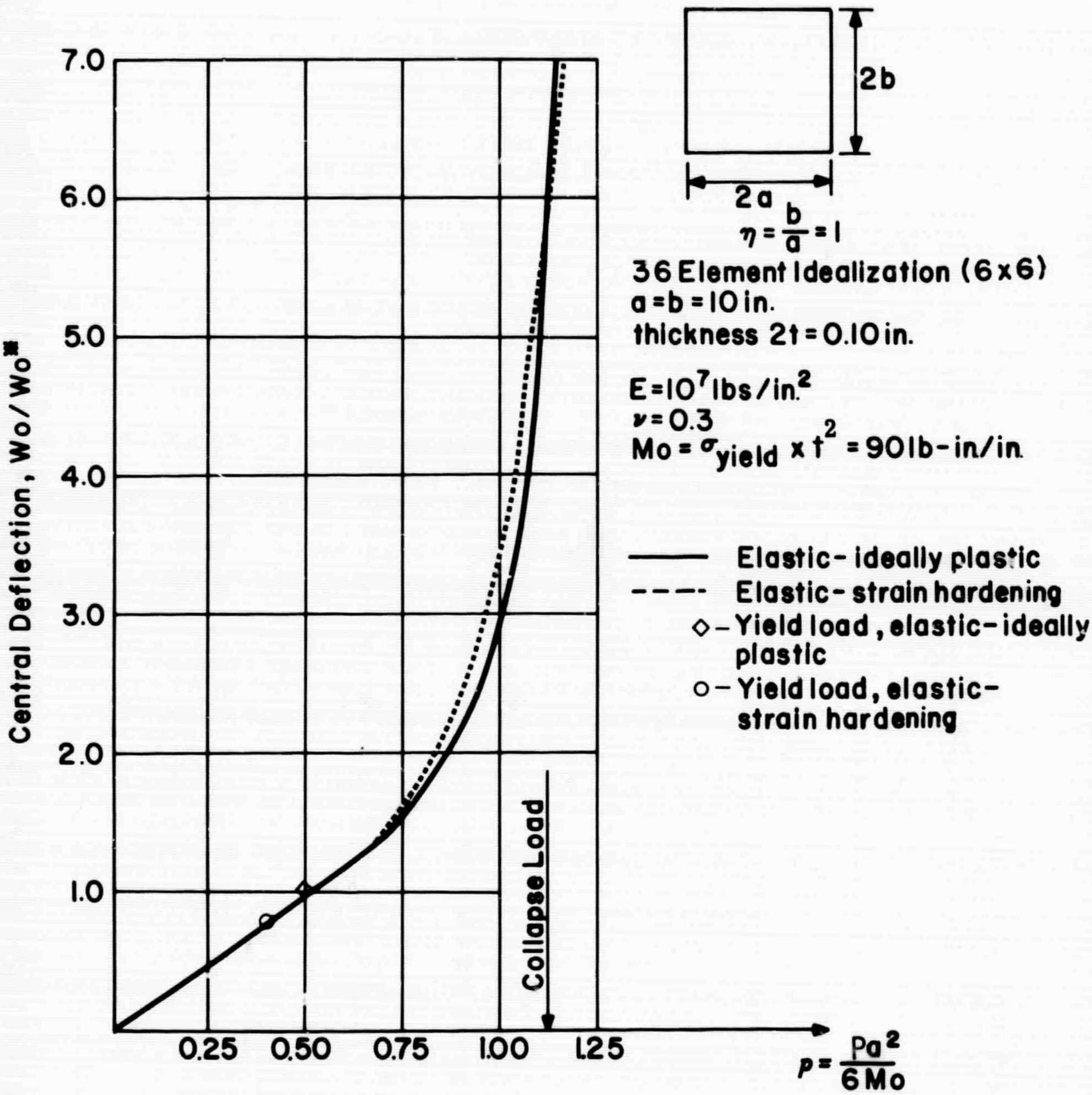

FIG.8 LOAD VERSUS CENTRAL DEFLECTION OF A UNIFORMLY LOADED SIMPLY SUPPORTED SQUARE PLATE

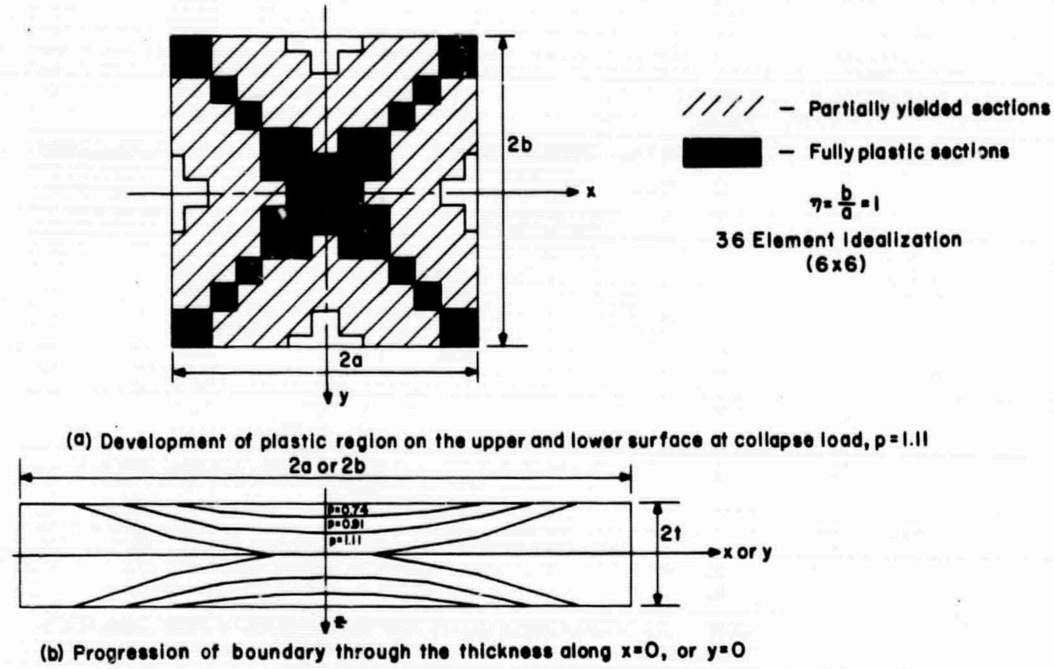

FIG. 9 PROGRESSION OF ELASTIC-PLASTIC REGION FOR SIMPLY SUPPORTED, UNIFORMLY LOADED SQUARE PLATE

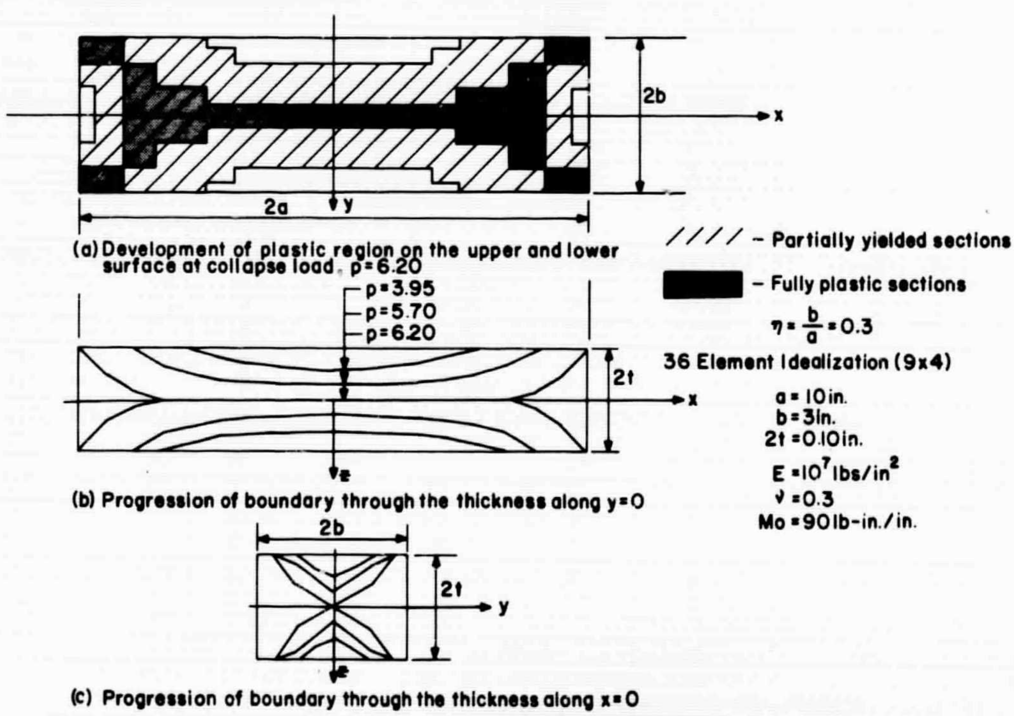

FIG. 10 PROGRESSION OF ELASTIC–PLASTIC REGION FOR SIMPLY SUPPORTED, UNIFORMLY LOADED RECTANGULAR PLATE

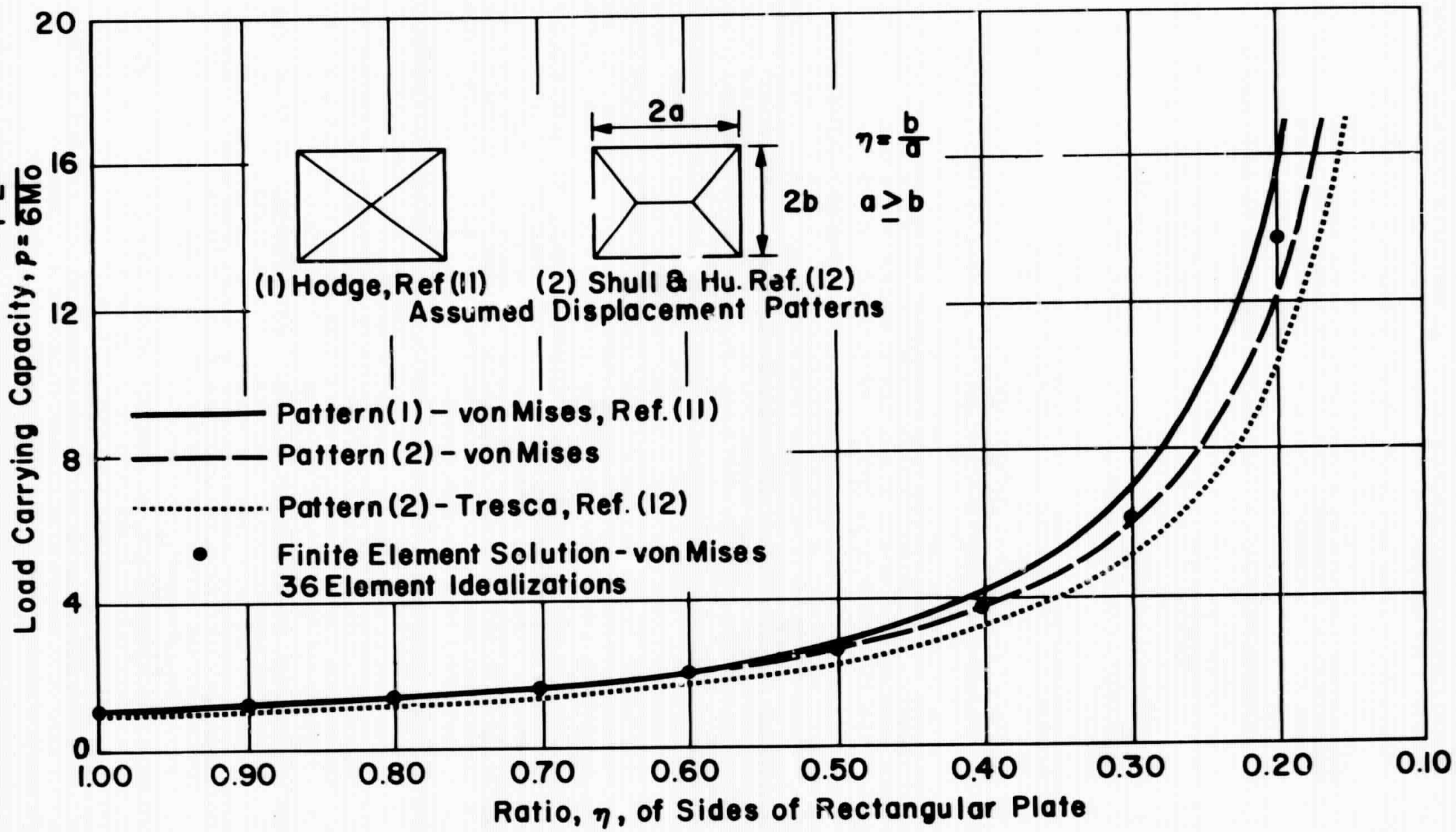

FIG. 11 COMPARISON OF UPPER BOUNDS ON LOAD CARRYING CAPACITIES OF RECTANGULAR PLATES

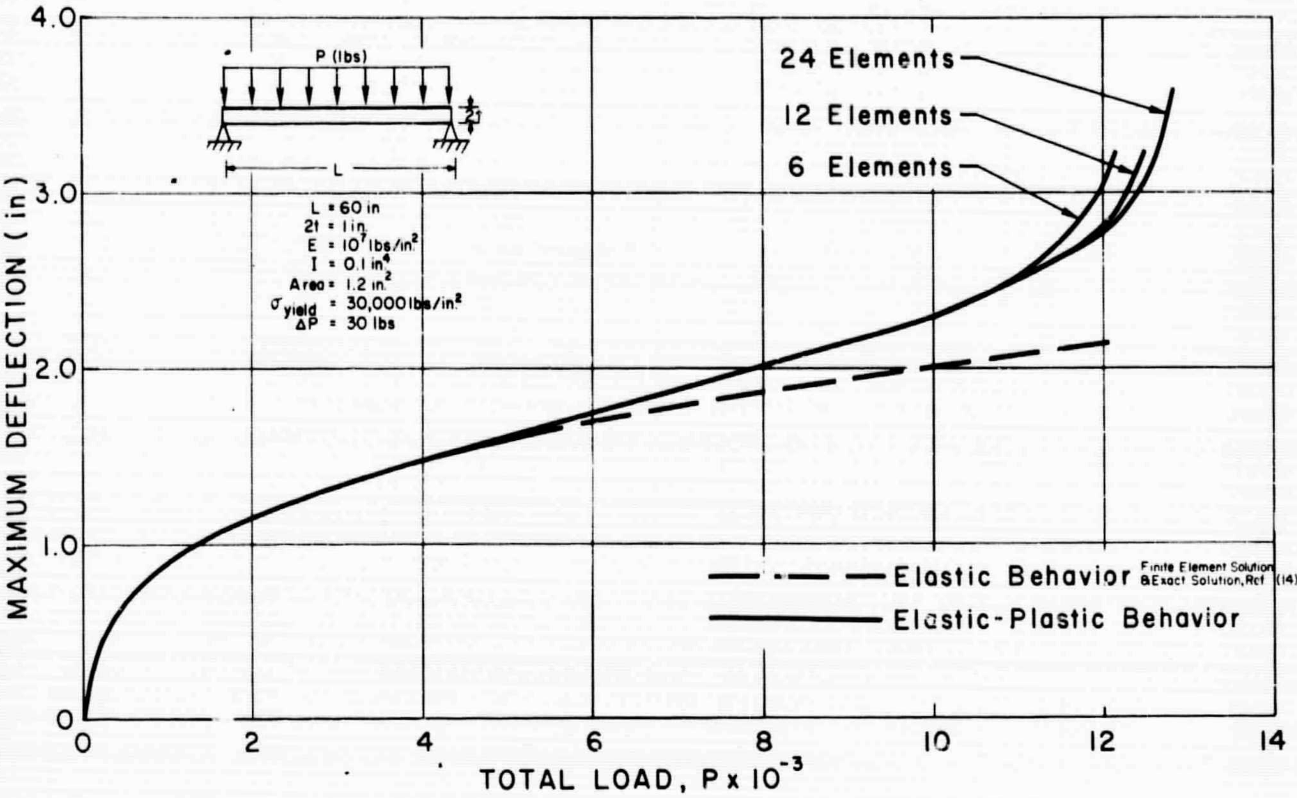

Fig. 12a ELASTIC-PLASTIC RESPONSE OF A RESTRAINED BEAM

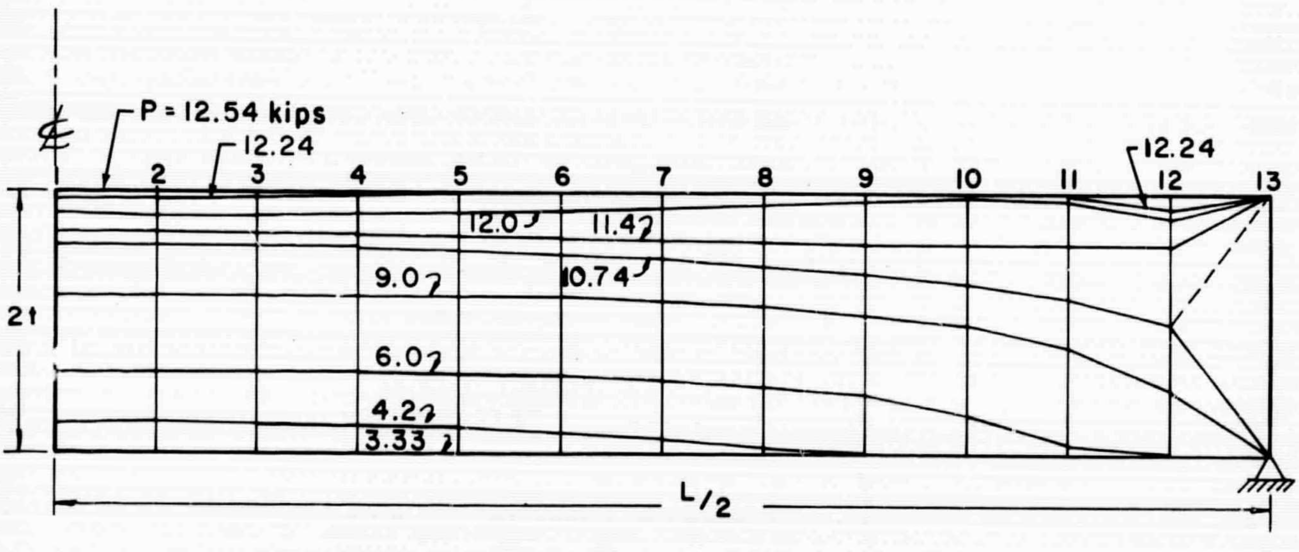

Fig. 12b PROGRESSION OF ELASTIC-PLASTIC BOUNDARY IN RESTRAINED BEAM FOR INCREASING LOAD

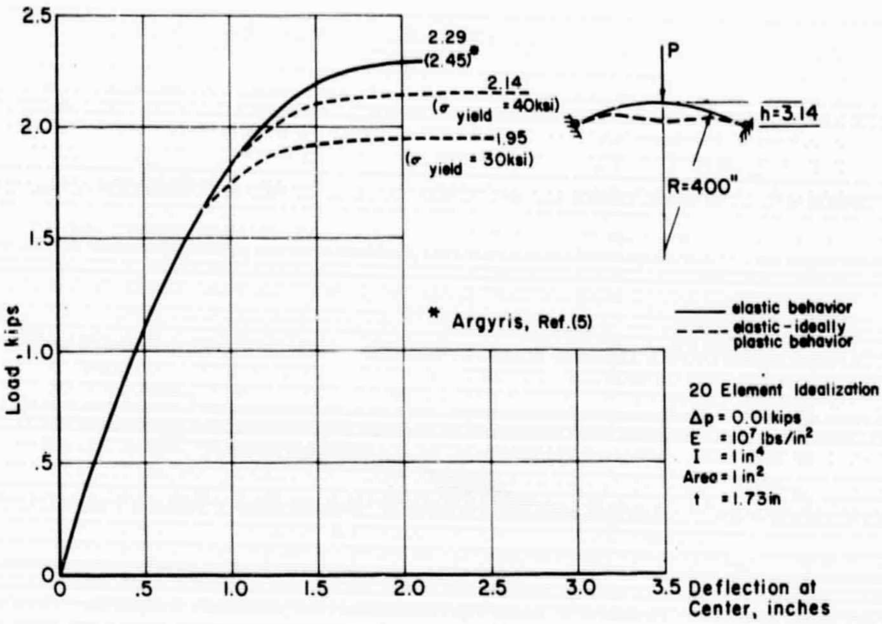

Fig. 13 LOAD VERSUS CENTRAL DEFLECTION FOR A SIMPLY SUPPORTED ARCH SUBJECTED TO A CONCENTRATED LOAD

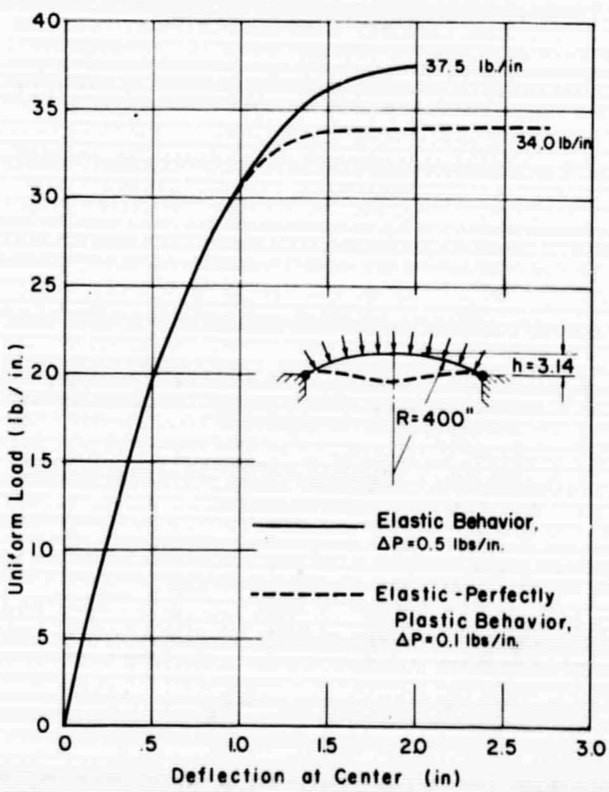

FIG. 14 LOAD VERSUS CENTRAL DEFLECTION OF A SIMPLY SUPPORTED ARCH SUBJECTED TO A UNIFORM LOAD

APPENDIX A

INITIAL STRAIN STIFFNESS MATRICES FOR BEAM FINITE ELEMENTS

The initial strain stiffness matrices for a beam element in pure bending, and for combined bending and membrane loading, are derived on the basis of the assumptions shown in Figs. 1 and 2, and are given in integral form in Eq. (10).

The matrix equation defining the fictitious nodal restoring forces in terms of the initial strain stiffness matrix is shown below for the pure bending of a beam with a rectangular cross section,

$$\begin{Bmatrix} P_{z_i} \\ M_i \\ P_{z_j} \\ M_j \end{Bmatrix} = \frac{EI}{t^3} \begin{bmatrix} c_1/\ell & c_2/\ell \\ c_3 & c_4 \\ -c_1/\ell & -c_2/\ell \\ c_5 & c_6 \end{bmatrix} \begin{Bmatrix} \epsilon_{0i} \\ \epsilon_{0j} \end{Bmatrix} = [k^*] \left\{\epsilon_0\right\} \tag{A-1}$$

where

$$c_1 = \frac{(\bar{z}_j - \bar{z}_i)^2}{20} + t^2 - \frac{\bar{z}_i(t + \bar{z}_i)}{2}$$

$$c_2 = \frac{9(\bar{z}_j - \bar{z}_i)^2}{20} + \frac{(\bar{z}_j - \bar{z}_i)(2\bar{z}_i + t)}{2} - t^2 + \frac{\bar{z}_i(t + \bar{z}_i)}{2}$$

$$c_3 = -\frac{(\bar{z}_j - \bar{z}_i)^2}{60} - \frac{(\bar{z}_j - \bar{z}_i)(2\bar{z}_i + t)}{12} + t^2 - \frac{\bar{z}_i(t + \bar{z}_i)}{2}$$

$$c_4 = \frac{(\bar{z}_j - \bar{z}_i)^2}{10} + \frac{(\bar{z}_j - \bar{z}_i)(2\bar{z}_i + t)}{12}$$

$$c_5 = \frac{(\bar{z}_j - \bar{z}_i)^2}{15} + \frac{(\bar{z}_j - \bar{z}_i)(2\bar{z}_i + t)}{12}$$

$$c_6 = \frac{7(\bar{z}_j - \bar{z}_i)^2}{20} + \frac{5(\bar{z}_j - \bar{z}_i)(2\bar{z}_i + t)}{12} - t^2 + \frac{\bar{z}_i(t + \bar{z}_i)}{2}$$

and P_z and M represent the fictitious restoring force in the lateral direction and moment, respectively. For this element, all $\bar{z}$'s are determined with respect to the median surface. Other quantities appearing in Eq. (A-1) are defined in Fig. 1.

The corresponding relation for the case of combined bending and membrane stresses is shown below:

$$\begin{Bmatrix} P_{z_i} \\ M_i \\ P_{x_i} \\ P_{z_j} \\ M_j \\ P_{x_j} \end{Bmatrix} = \frac{EI}{\ell^2 t^3} \begin{bmatrix} k^*_{11} & k^*_{12} & k^*_{13} & k^*_{14} \\ k^*_{21} & k^*_{22} & k^*_{23} & k^*_{24} \\ k^*_{31} & k^*_{32} & k^*_{33} & k^*_{34} \\ -k^*_{11} & -k^*_{12} & -k^*_{13} & -k^*_{14} \\ k^*_{51} & k^*_{52} & k^*_{53} & k^*_{54} \\ -k^*_{31} & -k^*_{32} & -k^*_{33} & -k^*_{34} \end{bmatrix} \begin{Bmatrix} \epsilon^U_{0i} \\ \epsilon^U_{0j} \\ \epsilon^L_{0i} \\ \epsilon^L_{0j} \end{Bmatrix} \qquad \text{(A-2)}$$

where

$$k_{11}^{*} = -(\ell^3/40)c_1 + (\ell/4)c_3$$

$$k_{12}^{*} = -(9\ell^3/40)c_1 - (\ell^2/4)c_2 - (\ell/4)c_3$$

$$k_{13}^{*} = -(\ell^3/40)c_4 + (\ell/4)c_6$$

$$k_{14}^{*} = -(9\ell^3/40)c_4 - (\ell^2/4)c_5 - (\ell/4)c_6$$

$$k_{21}^{*} = (\ell^4/120)c_1 + (\ell^3/24)c_2 + (\ell^2/4)c_3$$

$$k_{22}^{*} = -(\ell^4/20)c_1 - (\ell^3/24)c_2$$

$$k_{23}^{*} = (\ell^4/120)c_4 + (\ell^3/24)c_5 + (\ell^2/4)c_6$$

$$k_{24}^{*} = -(\ell^4/20)c_4 - (\ell^3/24)c_5$$

$$k_{31}^{*} = -(\ell^3/8)c_7 - (3\ell^2/8)c_8$$

$$k_{32}^{*} = -(\ell^3/4)c_7 - (3\ell^2/8)c_8$$

$$k_{33}^{*} = (\ell^3/8)c_9 + (3\ell^2/8)c_{10}$$

$$k_{34}^{*} = (\ell^3/4)c_9 + (3\ell^2/8)c_{10}$$

$$k_{51}^* = -\ (\ell^4/30)c_1 - (\ell^3/24)c_2$$

$$k_{52}^* = -\ (7\ell^4/40)c_1 - (5\ell^3/24)c_2 - (\ell^2/4)c_3$$

$$k_{53}^* = -\ (\ell^4/30)c_4 - (\ell^3/24)c_5$$

$$k_{54}^* = -\ (7\ell^4/40)c_4 - (5\ell^3/24)c_5 - (\ell^2/4)c_6$$

and

$$c_1 = \left(\bar{z}_j^U - \bar{z}_i^U\right)^2 \Big/ \ell^2$$

$$c_2 = -\left(\bar{z}_j^U - \bar{z}_i^U\right)\left(3t - 2\bar{z}_i^U\right) \Big/ \ell$$

$$c_3 = -\ \bar{z}_i^U \left(3t - \bar{z}_i^U\right)$$

$$c_4 = -\left(\bar{z}_j^L - \bar{z}_i^L\right)^2 \Big/ \ell^2$$

$$c_5 = \left(\bar{z}_j^L - \bar{z}_i^L\right)\left(t - 2\bar{z}_i^L\right) \Big/ \ell$$

$$c_6 = 2t^2 + t\bar{z}_i^L - \bar{z}_i^{L^2}$$

$$c_7 = \left(\bar{z}_j^U - \bar{z}_i^U\right) / \ell$$

$$c_8 = \bar{z}_i^U$$

$$c_9 = \left(\bar{z}_j^L - \bar{z}_i^L\right) / \ell$$

$$c_{10} = \bar{z}_i^L - 2t$$

The terms, P_{x_i} and P_{x_j}, represent the fictitious restoring forces in the axial direction. Here all $\bar{z}$'s are measured with respect to the upper surface of the beam. All other quantities appearing in Eq. (A-2) are defined in Fig. 2.

APPENDIX B

INITIAL STRAIN STIFFNESS MATRIX FOR RECTANGULAR PLATE ELEMENT

The initial strain stiffness matrix for a rectangular plate element in pure bending is derived on the basis of the assumptions shown in Fig. 3, and defined in integral form in Eq. (10).

$$\begin{Bmatrix} P_{z11} \\ M_{x11}/a \\ M_{y11}/b \\ M_{xy11}/ab \\ P_{z21} \\ \cdot \\ \cdot \\ \cdot \\ P_{z12} \\ \cdot \\ \cdot \\ \cdot \\ P_{z22} \\ M_{x22}/a \\ M_{y22}/b \\ M_{xy22}/ab \end{Bmatrix} = \frac{E}{3(1-\nu^2)} \underset{(16 \times 12)}{\Big[\; L(i,j) \;\Big]} \underset{(12 \times 12)}{\Big[\diagdown\; G \;\diagdown\Big]} \begin{Bmatrix} \epsilon_{x11} \\ \epsilon_{y11} \\ \gamma^{P}_{xy11} \\ \epsilon_{x21} \\ \cdot \\ \cdot \\ \cdot \\ \epsilon_{x12} \\ \cdot \\ \cdot \\ \cdot \\ \epsilon_{x22} \\ \epsilon_{y22} \\ \gamma^{P}_{xy22} \end{Bmatrix} = [k^*] \left\{\epsilon_0\right\} \qquad \text{(B-1)}$$

Here P_z and the M's represent the fictitious restoring force in the lateral direction and fictitious moments, respectively.

The matrix $\lceil G \rfloor$ is a diagonally partitioned array with 3 x 3 submatrices given by:

$$\begin{bmatrix} \frac{b}{a} & \nu \frac{b}{a} & 0 \\ \nu \frac{a}{b} & \frac{a}{b} & 0 \\ 0 & 0 & 1-\nu \end{bmatrix}$$

The coefficients of L(i,j) are given on the following pages, e.g.,

$$L(1,1) = (-7/20)(2t^2) + (4/15)t\bar{z}_{11} + (1/12)t\bar{z}_{12} + (0)t\bar{z}_{21}$$
$$+ (0)t\bar{z}_{22} + (27/140)\bar{z}_{11}^2 + (39/1400)\bar{z}_{12}^2 + (-3/140)\bar{z}_{21}^2$$
$$+ (-13/4200)\bar{z}_{22}^2 + (33/350)\bar{z}_{11}\bar{z}_{12} + (3/70)\bar{z}_{11}\bar{z}_{21}$$
$$+ (11/1050)\bar{z}_{11}\bar{z}_{22} + (11/1050)\bar{z}_{12}\bar{z}_{21}$$
$$+ (13/2100)\bar{z}_{12}\bar{z}_{22} + (-11/1050)\bar{z}_{21}\bar{z}_{22}$$

As in the case of pure bending of a beam all $\bar{z}$'s are measured with respect to the median surface. All other quantities appearing in Eq. (B-1) are defined in Fig. 3.

COEFFICIENTS OF L(I,J) FOR USE IN FORMING INITIAL STRAIN MATRIX

	(1,1)	(1,2)	(1,3)	(1,4)	(1,5)	(1,6)
Z * T**2	-7/ 20	-7/ 20	1/ 4	7/ 20	-3/ 20	1/ 4
T * Z11	4/ 15	4/ 15	-9/ 100	0/ 1	1/ 12	-3/ 50
T * Z12	1/ 12	0/ 1	-3/ 50	0/ 1	0/ 1	-1/ 25
T * Z21	0/ 1	1/ 12	-3/ 50	-4/ 15	1/ 15	-9/ 100
T * Z22	0/ 1	0/ 1	-1/ 25	-1/ 12	0/ 1	-3/ 50
Z11**2	27/ 140	27/ 140	-1/ 25	3/ 140	33/ 700	-1/ 50
Z12**2	39/ 1400	-3/ 140	-1/ 50	13/ 4200	-11/ 2100	-1/ 100
Z21**2	-3/ 140	39/ 1400	-1/ 50	-27/ 140	9/ 280	-1/ 25
Z22**2	-13/ 4200	-13/ 4200	-1/ 100	-39/ 1400	-1/ 280	-1/ 50
Z11 * Z12	33/ 350	3/ 70	-1/ 25	11/ 1050	11/ 1050	-1/ 50
Z11 * Z21	3/ 70	33/ 350	-1/ 25	-3/ 70	39/ 700	-1/ 25
Z11 * Z22	11/ 1050	11/ 1050	-1/ 50	-11/ 1050	13/ 2100	-1/ 50
Z12 * Z21	11/ 1050	11/ 1050	-1/ 50	-11/ 1050	13/ 2100	-1/ 50
Z12 * Z22	13/ 2100	-11/ 1050	-1/ 50	-13/ 2100	-13/ 2100	-1/ 50
Z21 * Z22	-11/ 1050	13/ 2100	-1/ 50	-33/ 350	1/ 140	-1/ 25

	(1,7)	(1,8)	(1,9)	(1,10)	(1,11)	(1,12)
Z * T**2	-3/ 20	7/ 20	1/ 4	3/ 20	3/ 20	1/ 4
T * Z11	1/ 12	0/ 1	-3/ 50	0/ 1	0/ 1	-1/ 25
T * Z12	1/ 15	-4/ 15	-9/ 100	0/ 1	-1/ 12	-3/ 50
T * Z21	0/ 1	0/ 1	-1/ 25	-1/ 12	0/ 1	-3/ 50
T * Z22	0/ 1	-1/ 12	-[illegible]/ 50	-1/ 15	-1/ 15	-9/ 100
Z11**2	33/ 700	3/ 140	-1/ 50	11/ 2100	11/ 2100	-1/ 100
Z12**2	9/ 280	-27/ 140	-1/ 25	1/ 280	-33/ 700	-1/ 50
Z21**2	-11/ 2100	13/ 4200	-1/ 100	-33/ 700	1/ 280	-1/ 50
Z22**2	-1/ 280	-39/ 1400	-1/ 50	-9/ 280	-9/ 280	-1/ 25
Z11 * Z12	39/ 700	-3/ 70	-1/ 25	13/ 2100	-11/ 1050	-1/ 50
Z11 * Z21	11/ 1050	11/ 1050	-1/ 50	-11/ 1050	13/ 2100	-1/ 50
Z11 * Z22	13/ 2100	-11/ 1050	-1/ 50	-13/ 2100	-13/ 2100	-1/ 50
Z12 * Z21	13/ 2100	-11/ 1050	-1/ 50	-13/ 2100	-13/ 2100	-1/ 50
Z12 * Z22	1/ 140	-33/ 350	-1/ 25	-1/ 140	-39/ 700	-1/ 25
Z21 * Z22	-13/ 2100	-13/ 2100	-1/ 50	-39/ 700	-1/ 140	-1/ 25

	(2,1)	(2,2)	(2,3)	(2,4)	(2,5)	(2,6)
Z * T**2	-7/ 20	-1/ 20	-1/ 24	0/ 1	-1/ 30	1/ 24
T * Z11	2/ 9	1/ 30	3/ 100	2/ 45	1/ 60	-1/ 200
T * Z12	5/ 72	0/ 1	1/ 50	1/ 72	0/ 1	-1/ 300
T * Z21	2/ 45	1/ 60	-1/ 200	-2/ 45	1/ 60	-1/ 50
T * Z22	1/ 72	0/ 1	-1/ 300	-1/ 72	0/ 1	-1/ 75
Z11**2	3/ 20	3/ 140	1/ 50	1/ 35	3/ 350	0/ 1
Z12**2	13/ 600	-1/ 420	1/ 100	13/ 3150	-1/ 1050	0/ 1
Z21**2	1/ 140	9/ 1400	-1/ 300	-3/ 70	3/ 350	-1/ 100
Z22**2	13/12600	-1/ 1400	-1/ 600	-13/ 2100	-1/ 1050	-1/ 200
Z11 * Z12	11/ 150	1/ 210	1/ 50	22/ 1575	1/ 525	0/ 1
Z11 * Z21	2/ 35	3/ 175	0/ 1	1/ 70	9/ 700	-1/ 150
Z11 * Z22	22/ 1575	1/ 525	0/ 1	11/ 3150	1/ 700	-1/ 300
Z12 * Z21	22/ 1575	1/ 525	0/ 1	11/ 3150	1/ 700	-1/ 300
Z12 * Z22	13/ 1575	-1/ 525	0/ 1	13/ 6300	-1/ 700	-1/ 300
Z21 * Z22	11/ 3150	1/ 700	-1/ 300	-11/ 525	1/ 525	-1/ 100

	(2,7)	(2,8)	(2,9)	(2,10)	(2,11)	(2,12)
Z * T**2	-3/ 20	1/ 20	-1/ 24	0/ 1	1/ 30	1/ 24
T * Z11	5/ 72	0/ 1	1/ 50	1/ 72	0/ 1	-1/ 300
T * Z12	1/ 18	-1/ 30	3/ 100	1/ 90	-1/ 60	-1/ 200
T * Z21	1/ 72	0/ 1	-1/ 300	-1/ 72	0/ 1	-1/ 75
T * Z22	1/ 90	-1/ 60	-1/ 200	-1/ 90	-1/ 60	-1/ 50
Z11**2	11/ 300	1/ 420	1/ 100	11/ 1575	1/ 1050	0/ 1
Z12**2	1/ 40	-3/ 140	1/ 50	1/ 210	-3/ 350	0/ 1
Z21**2	11/ 6300	1/ 1400	-1/ 600	-11/ 1050	1/ 1050	-1/ 200
Z22**2	1/ 840	-9/ 1400	-1/ 300	-1/ 140	-3/ 350	-1/ 100
Z11 * Z12	13/ 300	-1/ 210	1/ 50	13/ 1575	-1/ 525	0/ 1
Z11 * Z21	22/ 1575	1/ 525	0/ 1	11/ 3150	1/ 700	-1/ 300
Z11 * Z22	13/ 1575	-1/ 525	0/ 1	13/ 6300	-1/ 700	-1/ 300
Z12 * Z21	13/ 1575	-1/ 525	0/ 1	13/ 6300	-1/ 700	-1/ 300
Z12 * Z22	1/ 105	-3/ 175	0/ 1	1/ 420	-9/ 700	-1/ 150
Z21 * Z22	13/ 6300	-1/ 700	-1/ 300	-13/ 1050	-1/ 525	-1/ 100

COEFFICIENTS OF L(I,J) FOR USE IN FORMING INITIAL STRAIN MATRIX

	(3,1)	(3,2)	(3,3)	(3,4)	(3,5)	(3,6)
Z * T**2	-1/ 20	-7/ 20	-1/ 24	1/ 20	-3/ 20	-1/ 24
T * Z11	1/ 30	2/ 9	3/ 100	0/ 1	5/ 72	1/ 50
T * Z12	1/ 60	2/ 45	-1/ 200	0/ 1	1/ 72	-1/ 300
T * Z21	0/ 1	5/ 72	1/ 50	-1/ 30	1/ 18	3/ 100
T * Z22	0/ 1	1/ 72	-1/ 300	-1/ 60	1/ 90	-1/ 200
Z11**2	3/ 140	3/ 20	1/ 50	1/ 420	11/ 300	1/ 100
Z12**2	9/ 1400	1/ 140	-1/ 300	1/ 1400	11/ 6300	-1/ 600
Z21**2	-1/ 420	13/ 600	1/ 100	-3/ 140	1/ 40	1/ 50
Z22**2	-1/ 1400	13/12600	-1/ 600	-9/ 1400	1/ 840	-1/ 300
Z11 * Z12	3/ 175	2/ 35	0/ 1	1/ 525	22/ 1575	0/ 1
Z11 * Z21	1/ 210	11/ 150	1/ 50	-1/ 210	13/ 300	1/ 50
Z11 * Z22	1/ 525	22/ 1575	0/ 1	-1/ 525	13/ 1575	0/ 1
Z12 * Z21	1/ 525	22/ 1575	0/ 1	-1/ 525	13/ 1575	0/ 1
Z12 * Z22	1/ 700	11/ 3150	-1/ 300	-1/ 700	13/ 6300	-1/ 300
Z21 * Z22	-1/ 525	13/ 1575	0/ 1	-3/ 175	1/ 105	0/ 1

	(3,7)	(3,8)	(3,9)	(3,10)	(3,11)	(3,12)
Z * T**2	-1/ 30	0/ 1	1/ 24	1/ 30	0/ 1	1/ 24
T * Z11	1/ 60	2/ 45	-1/ 200	0/ 1	1/ 72	-1/ 300
T * Z12	1/ 60	-2/ 45	-1/ 50	0/ 1	-1/ 72	-1/ 75
T * Z21	0/ 1	1/ 72	-1/ 300	-1/ 60	1/ 90	-1/ 200
T * Z22	0/ 1	-1/ 72	-1/ 75	-1/ 60	-1/ 90	-1/ 50
Z11**2	3/ 350	1/ 35	0/ 1	1/ 1050	11/ 1575	0/ 1
Z12**2	3/ 350	-3/ 70	-1/ 100	1/ 1050	-11/ 1050	-1/ 200
Z21**2	-1/ 1050	13/ 3150	0/ 1	-3/ 350	1/ 210	0/ 1
Z22**2	-1/ 1050	-13/ 2100	-1/ 200	-3/ 350	-1/ 140	-1/ 100
Z11 * Z12	9/ 700	1/ 70	-1/ 150	1/ 700	11/ 3150	-1/ 300
Z11 * Z21	1/ 525	22/ 1575	0/ 1	-1/ 525	13/ 1575	0/ 1
Z11 * Z22	1/ 700	11/ 3150	-1/ 300	-1/ 700	13/ 6300	-1/ 300
Z12 * Z21	1/ 700	11/ 3150	-1/ 300	-1/ 700	13/ 6300	-1/ 300
Z12 * Z22	1/ 525	-11/ 525	-1/ 100	-1/ 525	-13/ 1050	-1/ 100
Z21 * Z22	-1/ 700	13/ 6300	-1/ 300	-9/ 700	1/ 420	-1/ 150

	(4,1)	(4,2)	(4,3)	(4,4)	(4,5)	(4,6)
Z * T**2	-1/ 20	-1/ 20	1/ 144	0/ 1	-1/ 30	-1/ 144
T * Z11	1/ 36	1/ 36	-1/ 100	1/ 180	1/ 72	1/ 600
T * Z12	1/ 72	1/ 180	1/ 600	1/ 360	1/ 360	-1/ 3600
T * Z21	1/ 180	1/ 72	1/ 600	-1/ 180	1/ 72	1/ 150
T * Z22	1/ 360	1/ 360	-1/ 3600	-1/ 360	1/ 360	-1/ 900
Z11**2	1/ 60	1/ 60	-1/ 100	1/ 315	1/ 150	0/ 1
Z12**2	1/ 200	1/ 1260	1/ 600	1/ 1050	1/ 3150	0/ 1
Z21**2	1/ 1260	1/ 200	1/ 600	-1/ 210	1/ 150	1/ 200
Z22**2	1/ 4200	1/ 4200	-1/ 3600	-1/ 700	1/ 3150	-1/ 1200
Z11 * Z12	1/ 75	2/ 315	0/ 1	4/ 1575	4/ 1575	0/ 1
Z11 * Z21	2/ 315	1/ 75	0/ 1	1/ 630	1/ 100	1/ 300
Z11 * Z22	4/ 1575	4/ 1575	0/ 1	1/ 1575	1/ 525	0/ 1
Z12 * Z21	4/ 1575	4/ 1575	0/ 1	1/ 1575	1/ 525	0/ 1
Z12 * Z22	1/ 525	1/ 1575	0/ 1	1/ 2100	1/ 2100	-1/ 1800
Z21 * Z22	1/ 1575	1/ 525	0/ 1	-2/ 525	4/ 1575	0/ 1

	(4,7)	(4,8)	(4,9)	(4,10)	(4,11)	(4,12)
Z * T**2	-1/ 30	0/ 1	-1/ 144	0/ 1	0/ 1	1/ 144
T * Z11	1/ 72	1/ 180	1/ 600	1/ 360	1/ 360	-1/ 3600
T * Z12	1/ 72	-1/ 180	1/ 150	1/ 360	-1/ 360	-1/ 900
T * Z21	1/ 360	1/ 360	-1/ 3600	-1/ 360	1/ 360	-1/ 900
T * Z22	1/ 360	-1/ 360	-1/ 900	-1/ 360	-1/ 360	-1/ 225
Z11**2	1/ 150	1/ 315	0/ 1	2/ 1575	2/ 1575	0/ 1
Z12**2	1/ 150	-1/ 210	1/ 200	2/ 1575	-1/ 525	0/ 1
Z21**2	1/ 3150	1/ 1050	0/ 1	-1/ 525	2/ 1575	0/ 1
Z22**2	1/ 3150	-1/ 700	-1/ 1200	-1/ 525	-1/ 525	-1/ 400
Z11 * Z12	1/ 100	1/ 630	1/ 300	1/ 525	1/ 1575	0/ 1
Z11 * Z21	4/ 1575	4/ 1575	0/ 1	1/ 1575	1/ 525	0/ 1
Z11 * Z22	1/ 525	1/ 1575	0/ 1	1/ 2100	1/ 2100	-1/ 1800
Z12 * Z21	1/ 525	1/ 1575	0/ 1	1/ 2100	1/ 2100	-1/ 1800
Z12 * Z22	4/ 1575	-2/ 525	0/ 1	1/ 1575	-1/ 350	-1/ 600
Z21 * Z22	1/ 2100	1/ 2100	-1/ 1800	-1/ 350	1/ 1575	-1/ 600

COEFFICIENTS OF L(I,J) FOR USE IN FORMING INITIAL STRAIN MATRIX

	(5,1)	(5,2)	(5,3)	(5,4)	(5,5)	(5,6)
L * T**2	7/ 20	-3/ 20	-1/ 4	-7/ 20	-7/ 20	-1/ 4
T * L11	-4/ 15	1/ 15	9/ 100	0/ 1	1/ 12	3/ 50
T * L12	-1/ 12	0/ 1	3/ 50	0/ 1	0/ 1	1/ 25
T * L21	0/ 1	1/ 12	3/ 50	4/ 15	4/ 15	9/ 100
T * L22	0/ 1	0/ 1	1/ 25	1/ 12	0/ 1	3/ 50
L11**2	-27/ 140	9/ 280	1/ 25	-3/ 140	39/ 1400	1/ 50
L12**2	-39/ 1400	-1/ 280	1/ 50	-13/ 4200	-13/ 4200	1/ 100
L21**2	3/ 140	33/ 700	1/ 50	27/ 140	27/ 140	1/ 25
L22**2	13/ 4200	-11/ 2100	1/ 100	39/ 1400	-3/ 140	1/ 50
L11 * L12	-33/ 350	1/ 140	1/ 25	-11/ 1050	13/ 2100	1/ 50
L11 * L21	-3/ 70	39/ 700	1/ 25	3/ 70	33/ 350	1/ 25
L11 * L22	-11/ 1050	13/ 2100	1/ 50	11/ 1050	11/ 1050	1/ 50
L12 * L21	-11/ 1050	13/ 2100	1/ 50	11/ 1050	11/ 1050	1/ 50
L12 * L22	-13/ 2100	-13/ 2100	1/ 50	13/ 2100	-11/ 1050	1/ 50
L21 * L22	11/ 1050	11/ 1050	1/ 50	33/ 350	3/ 70	1/ 25

	(5,7)	(5,8)	(5,9)	(5,10)	(5,11)	(5,12)
L * T**2	3/ 20	3/ 20	-1/ 4	-3/ 20	7/ 20	-1/ 4
T * L11	-1/ 12	0/ 1	3/ 50	0/ 1	0/ 1	1/ 25
T * L12	-1/ 15	-1/ 15	9/ 100	0/ 1	-1/ 12	3/ 50
T * L21	0/ 1	0/ 1	1/ 25	1/ 12	0/ 1	3/ 50
T * L22	0/ 1	-1/ 12	3/ 50	1/ 15	-4/ 15	9/ 100
L11**2	-33/ 700	1/ 280	1/ 50	-11/ 2100	13/ 4200	1/ 100
L12**2	-9/ 280	-9/ 280	1/ 25	-1/ 280	-39/ 1400	1/ 50
L21**2	11/ 2100	11/ 2100	1/ 100	33/ 700	3/ 140	1/ 50
L22**2	1/ 280	-33/ 700	1/ 50	9/ 280	-27/ 140	1/ 25
L11 * L12	-39/ 700	-1/ 140	1/ 25	-13/ 2100	-13/ 2100	1/ 50
L11 * L21	-11/ 1050	13/ 2100	1/ 50	11/ 1050	11/ 1050	1/ 50
L11 * L22	-13/ 2100	-13/ 2100	1/ 50	13/ 2100	-11/ 1050	1/ 50
L12 * L21	-13/ 2100	-13/ 2100	1/ 50	13/ 2100	-11/ 1050	1/ 50
L12 * L22	-1/ 140	-39/ 700	1/ 25	1/ 140	-33/ 350	1/ 25
L21 * L22	13/ 2100	-11/ 1050	1/ 50	39/ 700	-3/ 70	1/ 25

	(6,1)	(6,2)	(6,3)	(6,4)	(6,5)	(6,6)
L * T**2	0/ 1	1/ 30	1/ 24	7/ 20	1/ 20	-1/ 24
T * L11	2/ 45	-1/ 60	-1/ 50	-2/ 45	-1/ 60	-1/ 200
T * L12	1/ 72	0/ 1	-1/ 75	-1/ 72	0/ 1	-1/ 300
T * L21	-2/ 45	-1/ 60	-1/ 200	-2/ 9	-1/ 30	3/ 100
T * L22	-1/ 72	0/ 1	-1/ 300	-5/ 72	0/ 1	1/ 50
L11**2	3/ 70	-3/ 350	-1/ 100	-1/ 140	-9/ 1400	-1/ 300
L12**2	13/ 2100	1/ 1050	-1/ 200	-13/12600	1/ 1400	-1/ 600
L21**2	-1/ 35	-3/ 350	0/ 1	-3/ 20	-3/ 140	1/ 50
L22**2	-13/ 3150	1/ 1050	0/ 1	-13/ 600	1/ 420	1/ 100
L11 * L12	11/ 525	-1/ 525	-1/ 100	-11/ 3150	-1/ 700	-1/ 300
L11 * L21	-1/ 70	-9/ 700	-1/ 150	-2/ 35	-3/ 175	0/ 1
L11 * L22	-11/ 3150	-1/ 700	-1/ 300	-22/ 1575	-1/ 525	0/ 1
L12 * L21	-11/ 3150	-1/ 700	-1/ 300	-22/ 1575	-1/ 525	0/ 1
L12 * L22	-13/ 6300	1/ 700	-1/ 300	-13/ 1575	1/ 525	0/ 1
L21 * L22	-22/ 1575	-1/ 525	0/ 1	-11/ 150	-1/ 210	1/ 50

	(6,7)	(6,8)	(6,9)	(6,10)	(6,11)	(6,12)
L * T**2	0/ 1	-1/ 30	1/ 24	3/ 20	-1/ 20	-1/ 24
T * L11	1/ 72	0/ 1	-1/ 75	-1/ 72	0/ 1	-1/ 300
T * L12	1/ 90	1/ 60	-1/ 50	-1/ 90	1/ 60	-1/ 200
T * L21	-1/ 72	0/ 1	-1/ 300	-5/ 72	0/ 1	1/ 50
T * L22	-1/ 90	1/ 60	-1/ 200	-1/ 18	1/ 30	3/ 100
L11**2	11/ 1050	-1/ 1050	-1/ 200	-11/ 6300	-1/ 1400	-1/ 600
L12**2	1/ 140	3/ 350	-1/ 100	-1/ 840	9/ 1400	-1/ 300
L21**2	-11/ 1575	-1/ 1050	0/ 1	-11/ 300	-1/ 420	1/ 100
L22**2	-1/ 210	3/ 350	0/ 1	-1/ 40	3/ 140	1/ 50
L11 * L12	13/ 1050	1/ 525	-1/ 100	-13/ 6300	1/ 700	-1/ 300
L11 * L21	-11/ 3150	-1/ 700	-1/ 300	-22/ 1575	-1/ 525	0/ 1
L11 * L22	-13/ 6300	1/ 700	-1/ 300	-13/ 1575	1/ 525	0/ 1
L12 * L21	-13/ 6300	1/ 700	-1/ 300	-13/ 1575	1/ 525	0/ 1
L12 * L22	-1/ 420	9/ 700	-1/ 150	-1/ 105	3/ 175	0/ 1
L21 * L22	-13/ 1575	1/ 525	0/ 1	-13/ 300	1/ 210	1/ 50

COEFFICIENTS OF L(I,J) FOR USE IN FORMING INITIAL STRAIN MATRIX

	(7,1)	(7,2)	(7,3)	(7,4)	(7,5)	(7,6)
2 * T**2	1/ 20	-3/ 20	1/ 24	-1/ 20	-7/ 20	1/ 24
T * L11	-1/ 30	1/ 18	-3/ 100	0/ 1	5/ 72	-1/ 50
T * L12	-1/ 60	1/ 90	1/ 200	0/ 1	1/ 72	1/ 300
T * L21	0/ 1	5/ 72	-1/ 50	1/ 30	2/ 9	-3/ 100
T * L22	0/ 1	1/ 72	1/ 300	1/ 60	2/ 45	1/ 200
L11**2	-3/ 140	1/ 40	-1/ 50	-1/ 420	13/ 600	-1/ 100
L12**2	-9/ 1400	1/ 840	1/ 300	-1/ 1400	13/12600	1/ 600
L21**2	1/ 420	11/ 300	-1/ 100	3/ 140	3/ 20	-1/ 50
L22**2	1/ 1400	11/ 6300	1/ 600	9/ 1400	1/ 140	1/ 300
L11 * L12	-3/ 175	1/ 105	0/ 1	-1/ 525	13/ 1575	0/ 1
L11 * L21	-1/ 210	13/ 300	-1/ 50	1/ 210	11/ 150	-1/ 50
L11 * L22	-1/ 525	13/ 1575	0/ 1	1/ 525	22/ 1575	0/ 1
L12 * L21	-1/ 525	13/ 1575	0/ 1	1/ 525	22/ 1575	0/ 1
L12 * L22	-1/ 700	13/ 6300	1/ 300	1/ 700	11/ 3150	1/ 300
L21 * L22	1/ 525	22/ 1575	0/ 1	3/ 175	2/ 35	0/ 1

	(7,7)	(7,8)	(7,9)	(7,10)	(7,11)	(7,12)
2 * T**2	1/ 30	0/ 1	-1/ 24	-1/ 30	0/ 1	-1/ 24
T * L11	-1/ 60	1/ 90	1/ 200	0/ 1	1/ 72	1/ 300
T * L12	-1/ 60	-1/ 90	1/ 50	0/ 1	-1/ 72	1/ 75
T * L21	0/ 1	1/ 72	1/ 300	1/ 60	2/ 45	1/ 200
T * L22	0/ 1	-1/ 72	1/ 75	1/ 60	-2/ 45	1/ 50
L11**2	-3/ 350	1/ 210	0/ 1	-1/ 1050	13/ 3150	0/ 1
L12**2	-3/ 350	-1/ 140	1/ 100	-1/ 1050	-13/ 2100	1/ 200
L21**2	1/ 1050	11/ 1575	0/ 1	3/ 350	1/ 35	0/ 1
L22**2	1/ 1050	-11/ 1050	1/ 200	3/ 350	-3/ 70	1/ 100
L11 * L12	-9/ 700	1/ 420	1/ 150	-1/ 700	13/ 6300	1/ 300
L11 * L21	-1/ 525	13/ 1575	0/ 1	1/ 525	22/ 1575	0/ 1
L11 * L22	-1/ 700	13/ 6300	1/ 300	1/ 700	11/ 3150	1/ 300
L12 * L21	-1/ 700	13/ 6300	1/ 300	1/ 700	11/ 3150	1/ 300
L12 * L22	-1/ 525	-13/ 1050	1/ 100	1/ 525	-11/ 525	1/ 100
L21 * L22	1/ 700	11/ 3150	1/ 300	9/ 700	1/ 70	1/ 150

	(8,1)	(8,2)	(8,3)	(8,4)	(8,5)	(8,6)
2 * T**2	0/ 1	1/ 30	-1/ 144	1/ 20	1/ 20	1/ 144
T * L11	1/ 180	-1/ 72	1/ 150	-1/ 180	-1/ 72	1/ 600
T * L12	1/ 360	-1/ 360	-1/ 900	-1/ 360	-1/ 360	-1/ 3600
T * L21	-1/ 180	-1/ 72	1/ 600	-1/ 36	-1/ 36	-1/ 100
T * L22	-1/ 360	-1/ 360	-1/ 3600	-1/ 72	-1/ 180	1/ 600
L11**2	1/ 210	-1/ 150	1/ 200	-1/ 1260	-1/ 200	1/ 600
L12**2	1/ 700	-1/ 3150	-1/ 1200	-1/ 4200	-1/ 4200	-1/ 3600
L21**2	-1/ 315	-1/ 150	0/ 1	-1/ 60	-1/ 60	-1/ 100
L22**2	-1/ 1050	-1/ 3150	0/ 1	-1/ 200	-1/ 1260	1/ 600
L11 * L12	2/ 525	-4/ 1575	0/ 1	-1/ 1575	-1/ 525	0/ 1
L11 * L21	-1/ 630	-1/ 100	1/ 300	-2/ 315	-1/ 75	0/ 1
L11 * L22	-1/ 1575	-1/ 525	0/ 1	-4/ 1575	-4/ 1575	0/ 1
L12 * L21	-1/ 1575	-1/ 525	0/ 1	-4/ 1575	-4/ 1575	0/ 1
L12 * L22	-1/ 2100	-1/ 2100	-1/ 1800	-1/ 525	-1/ 1575	0/ 1
L21 * L22	-4/ 1575	-4/ 1575	0/ 1	-1/ 75	-2/ 315	0/ 1

	(8,7)	(8,8)	(8,9)	(8,10)	(8,11)	(8,12)
2 * T**2	0/ 1	0/ 1	1/ 144	1/ 30	0/ 1	-1/ 144
T * L11	1/ 360	-1/ 360	-1/ 900	-1/ 360	-1/ 360	-1/ 3600
T * L12	1/ 360	1/ 360	-1/ 225	-1/ 360	1/ 360	-1/ 900
T * L21	-1/ 360	-1/ 360	-1/ 3600	-1/ 72	-1/ 180	1/ 600
T * L22	-1/ 360	1/ 360	-1/ 900	-1/ 72	1/ 180	1/ 150
L11**2	1/ 525	-2/ 1575	0/ 1	-1/ 3150	-1/ 1050	0/ 1
L12**2	1/ 525	1/ 525	-1/ 400	-1/ 3150	1/ 700	-1/ 1200
L21**2	-2/ 1575	-2/ 1575	0/ 1	-1/ 150	-1/ 315	0/ 1
L22**2	-2/ 1575	1/ 525	0/ 1	-1/ 150	1/ 210	1/ 200
L11 * L12	1/ 350	-1/ 1575	-1/ 600	-1/ 2100	-1/ 2100	-1/ 1800
L11 * L21	-1/ 1575	-1/ 525	0/ 1	-4/ 1575	-4/ 1575	0/ 1
L11 * L22	-1/ 2100	-1/ 2100	-1/ 1800	-1/ 525	-1/ 1575	0/ 1
L12 * L21	-1/ 2100	-1/ 2100	-1/ 1800	-1/ 525	-1/ 1575	0/ 1
L12 * L22	-1/ 1575	1/ 350	-1/ 600	-4/ 1575	2/ 525	0/ 1
L21 * L22	-1/ 525	-1/ 1575	0/ 1	-1/ 100	-1/ 630	1/ 300

COEFFICIENTS OF L(I,J) FOR USE IN FORMING INITIAL STRAIN MATRIX

	(9,1)	(9,2)	(9,3)	(9,4)	(9,5)	(9,6)
L * T**2	-3/ 20	7/ 20	-1/ 4	3/ 20	3/ 20	-1/ 4
T * L11	1/ 15	-4/ 15	9/ 100	0/ 1	-1/ 12	3/ 50
T * L12	1/ 12	0/ 1	3/ 50	0/ 1	0/ 1	1/ 25
T * L21	0/ 1	-1/ 12	3/ 50	-1/ 15	-1/ 15	9/ 100
T * L22	0/ 1	0/ 1	1/ 25	-1/ 12	0/ 1	3/ 50
L11**2	9/ 280	-27/ 140	1/ 25	1/ 280	-33/ 700	1/ 50
L12**2	33/ 700	3/ 140	1/ 50	11/ 2100	11/ 2100	1/ 100
L21**2	-1/ 280	-39/ 1400	1/ 50	-9/ 280	-9/ 280	1/ 25
L22**2	-11/ 2100	13/ 4200	1/ 100	-33/ 700	1/ 280	1/ 50
L11 * L12	39/ 700	-3/ 70	1/ 25	13/ 2100	-11/ 1050	1/ 50
L11 * L21	1/ 140	-33/ 350	1/ 25	-1/ 140	-39/ 700	1/ 25
L11 * L22	13/ 2100	-11/ 1050	1/ 50	-13/ 2100	-13/ 2100	1/ 50
L12 * L21	13/ 2100	-11/ 1050	1/ 50	-13/ 2100	-13/ 2100	1/ 50
L12 * L22	11/ 1050	11/ 1050	1/ 50	-11/ 1050	13/ 2100	1/ 50
L21 * L22	-13/ 2100	-13/ 2100	1/ 50	-39/ 700	-1/ 140	1/ 25

	(9,7)	(9,8)	(9,9)	(9,10)	(9,11)	(9,12)
L * T**2	-7/ 20	-7/ 20	-1/ 4	7/ 20	-3/ 20	-1/ 4
T * L11	1/ 12	0/ 1	3/ 50	0/ 1	0/ 1	1/ 25
T * L12	4/ 15	4/ 15	9/ 100	0/ 1	1/ 12	3/ 50
T * L21	0/ 1	0/ 1	1/ 25	-1/ 12	0/ 1	3/ 50
T * L22	0/ 1	1/ 12	3/ 50	-4/ 15	1/ 15	9/ 100
L11**2	39/ 1400	-3/ 140	1/ 50	13/ 4200	-11/ 2100	1/ 100
L12**2	27/ 140	27/ 140	1/ 25	3/ 140	33/ 700	1/ 50
L21**2	-13/ 4200	-13/ 4200	1/ 100	-39/ 1400	-1/ 280	1/ 50
L22**2	-3/ 140	39/ 1400	1/ 50	-27/ 140	9/ 280	1/ 25
L11 * L12	33/ 350	3/ 70	1/ 25	11/ 1050	11/ 1050	1/ 50
L11 * L21	13/ 2100	-11/ 1050	1/ 50	-13/ 2100	-13/ 2100	1/ 50
L11 * L22	11/ 1050	11/ 1050	1/ 50	-11/ 1050	13/ 2100	1/ 50
L12 * L21	11/ 1050	11/ 1050	1/ 50	-11/ 1050	13/ 2100	1/ 50
L12 * L22	3/ 70	33/ 350	1/ 25	-3/ 70	39/ 700	1/ 25
L21 * L22	-11/ 1050	13/ 2100	1/ 50	-33/ 350	1/ 140	1/ 25

	(10,1)	(10,2)	(10,3)	(10,4)	(10,5)	(10,6)
L * T**2	-3/ 20	1/ 20	1/ 24	0/ 1	1/ 30	-1/ 24
T * L11	1/ 18	-1/ 30	-3/ 100	1/ 90	-1/ 60	1/ 200
T * L12	5/ 72	0/ 1	-1/ 50	1/ 72	0/ 1	1/ 300
T * L21	1/ 90	-1/ 60	1/ 200	-1/ 90	-1/ 60	1/ 50
T * L22	1/ 72	0/ 1	1/ 300	-1/ 72	0/ 1	1/ 75
L11**2	1/ 40	-3/ 140	-1/ 50	1/ 210	-3/ 350	0/ 1
L12**2	11/ 300	1/ 420	-1/ 100	11/ 1575	1/ 1050	0/ 1
L21**2	1/ 840	-9/ 1400	1/ 300	-1/ 140	-3/ 350	1/ 100
L22**2	11/ 6300	1/ 1400	1/ 600	-11/ 1050	1/ 1050	1/ 200
L11 * L12	13/ 300	-1/ 210	-1/ 50	13/ 1575	-1/ 525	0/ 1
L11 * L21	1/ 105	-3/ 175	0/ 1	1/ 420	-9/ 700	1/ 150
L11 * L22	13/ 1575	-1/ 525	0/ 1	13/ 6300	-1/ 700	1/ 300
L12 * L21	13/ 1575	-1/ 525	0/ 1	13/ 6300	-1/ 700	1/ 300
L12 * L22	22/ 1575	1/ 525	0/ 1	11/ 3150	1/ 700	1/ 300
L21 * L22	13/ 6300	-1/ 700	1/ 300	-13/ 1050	-1/ 525	1/ 100

	(10,7)	(10,8)	(10,9)	(10,10)	(10,11)	(10,12)
L * T**2	-7/ 20	-1/ 20	1/ 24	0/ 1	-1/ 30	-1/ 24
T * L11	5/ 72	0/ 1	-1/ 50	1/ 72	0/ 1	1/ 300
T * L12	2/ 9	1/ 30	-3/ 100	2/ 45	1/ 60	1/ 200
T * L21	1/ 72	0/ 1	1/ 300	-1/ 72	0/ 1	1/ 75
T * L22	2/ 45	1/ 60	1/ 200	-2/ 45	1/ 60	1/ 50
L11**2	13/ 600	-1/ 420	-1/ 100	13/ 3150	-1/ 1050	0/ 1
L12**2	3/ 20	3/ 140	-1/ 50	1/ 35	3/ 350	0/ 1
L21**2	13/12600	-1/ 1400	1/ 600	-13/ 2100	-1/ 1050	1/ 200
L22**2	1/ 140	9/ 1400	1/ 300	-3/ 70	3/ 350	1/ 100
L11 * L12	11/ 150	1/ 210	-1/ 50	22/ 1575	1/ 525	0/ 1
L11 * L21	13/ 1575	-1/ 525	0/ 1	13/ 6300	-1/ 700	1/ 300
L11 * L22	22/ 1575	1/ 525	0/ 1	11/ 3150	1/ 700	1/ 300
L12 * L21	22/ 1575	1/ 525	0/ 1	11/ 3150	1/ 700	1/ 300
L12 * L22	2/ 35	3/ 175	0/ 1	1/ 70	9/ 700	1/ 150
L21 * L22	11/ 3150	1/ 700	1/ 300	-11/ 525	1/ 525	1/ 100

COEFFICIENTS OF L(I,J) FOR USE IN FORMING INITIAL STRAIN MATRIX

	(11,1)	(11,2)	(11,3)	(11,4)	(11,5)	(11,6)
ℓ * T**2	1/ 30	0/ 1	1/ 24	-1/ 30	0/ 1	1/ 24
T * ℓ11	-1/ 60	2/ 45	-1/ 50	0/ 1	1/ 72	-1/ 75
T * ℓ12	-1/ 60	-2/ 45	-1/ 200	0/ 1	-1/ 72	-1/ 300
T * ℓ21	0/ 1	1/ 72	-1/ 75	1/ 60	1/ 90	-1/ 50
T * ℓ22	0/ 1	-1/ 72	-1/ 300	1/ 60	-1/ 90	-1/ 200
ℓ11**2	3/ 350	3/ 70	-1/ 100	-1/ 1050	11/ 1050	-1/ 200
ℓ12**2	-3/ 350	-1/ 35	0/ 1	-1/ 1050	-11/ 1575	0/ 1
ℓ21**2	1/ 1050	13/ 2100	-1/ 200	3/ 350	1/ 140	-1/ 100
ℓ22**2	1/ 1050	-13/ 3150	0/ 1	3/ 350	-1/ 210	0/ 1
ℓ11 * ℓ12	-9/ 700	-1/ 70	-1/ 150	-1/ 700	-11/ 3150	-1/ 300
ℓ11 * ℓ21	-1/ 525	11/ 525	-1/ 100	1/ 525	13/ 1050	-1/ 100
ℓ11 * ℓ22	-1/ 700	-11/ 3150	-1/ 300	1/ 700	-13/ 6300	-1/ 300
ℓ12 * ℓ21	-1/ 700	-11/ 3150	-1/ 300	1/ 700	-13/ 6300	-1/ 300
ℓ12 * ℓ22	-1/ 525	-22/ 1575	0/ 1	1/ 525	-13/ 1575	0/ 1
ℓ21 * ℓ22	1/ 700	-13/ 6300	-1/ 300	9/ 700	-1/ 420	-1/ 150

	(11,7)	(11,8)	(11,9)	(11,10)	(11,11)	(11,12)
ℓ * T**2	1/ 20	7/ 20	-1/ 24	-1/ 20	3/ 20	-1/ 24
T * ℓ11	-1/ 60	-2/ 45	-1/ 200	0/ 1	-1/ 72	-1/ 300
T * ℓ12	-1/ 30	-2/ 9	3/ 100	0/ 1	-5/ 72	1/ 50
T * ℓ21	0/ 1	-1/ 72	-1/ 300	1/ 60	-1/ 90	-1/ 200
T * ℓ22	0/ 1	-5/ 72	1/ 50	1/ 30	-1/ 18	3/ 100
ℓ11**2	-9/ 1400	-1/ 140	-1/ 300	-1/ 1400	-11/ 6300	-1/ 600
ℓ12**2	-3/ 140	-3/ 20	1/ 50	-1/ 420	-11/ 300	1/ 100
ℓ21**2	1/ 1400	-13/12600	-1/ 600	9/ 1400	-1/ 840	-1/ 300
ℓ22**2	1/ 420	-13/ 600	1/ 100	3/ 140	-1/ 40	1/ 50
ℓ11 * ℓ12	-3/ 175	-2/ 35	0/ 1	-1/ 525	-22/ 1575	0/ 1
ℓ11 * ℓ21	-1/ 700	-11/ 3150	-1/ 300	1/ 700	-13/ 6300	-1/ 300
ℓ11 * ℓ22	-1/ 525	-22/ 1575	0/ 1	1/ 525	-13/ 1575	0/ 1
ℓ12 * ℓ21	-1/ 525	-22/ 1575	0/ 1	1/ 525	-13/ 1575	0/ 1
ℓ12 * ℓ22	-1/ 210	-11/ 150	1/ 50	1/ 210	-13/ 300	1/ 50
ℓ21 * ℓ22	1/ 525	-13/ 1575	0/ 1	3/ 175	-1/ 105	0/ 1

	(12,1)	(12,2)	(12,3)	(12,4)	(12,5)	(12,6)
ℓ * T**2	1/ 30	0/ 1	-1/ 144	0/ 1	0/ 1	1/ 144
T * ℓ11	-1/ 72	1/ 180	1/ 150	-1/ 360	1/ 360	-1/ 300
T * ℓ12	-1/ 72	-1/ 180	1/ 600	-1/ 360	-1/ 360	-1/ 3600
T * ℓ21	-1/ 360	1/ 360	-1/ 900	1/ 360	-1/ 360	-1/ 225
T * ℓ22	-1/ 360	-1/ 360	-1/ 3600	1/ 360	-1/ 360	-1/ 900
ℓ11**2	-1/ 150	1/ 210	1/ 200	-2/ 1575	1/ 525	0/ 1
ℓ12**2	-1/ 150	-1/ 315	0/ 1	-2/ 1575	-2/ 1575	0/ 1
ℓ21**2	-1/ 3150	1/ 700	-1/ 1200	1/ 525	1/ 525	-1/ 400
ℓ22**2	-1/ 3150	-1/ 1050	0/ 1	1/ 525	-2/ 1575	0/ 1
ℓ11 * ℓ12	-1/ 100	-1/ 630	1/ 300	-1/ 525	-1/ 1575	0/ 1
ℓ11 * ℓ21	-4/ 1575	2/ 525	0/ 1	-1/ 1575	1/ 350	-1/ 600
ℓ11 * ℓ22	-1/ 525	-1/ 1575	0/ 1	-1/ 2100	-1/ 2100	-1/ 1800
ℓ12 * ℓ21	-1/ 525	-1/ 1575	0/ 1	-1/ 2100	-1/ 2100	-1/ 1800
ℓ12 * ℓ22	-4/ 1575	-4/ 1575	0/ 1	-1/ 1575	-1/ 525	0/ 1
ℓ21 * ℓ22	-1/ 2100	-1/ 2100	-1/ 1800	1/ 350	-1/ 1575	-1/ 600

	(12,7)	(12,8)	(12,9)	(12,10)	(12,11)	(12,12)
ℓ * T**2	1/ 20	1/ 20	1/ 144	0/ 1	1/ 30	-1/ 144
T * ℓ11	-1/ 72	-1/ 180	1/ 600	-1/ 360	-1/ 360	-1/ 3600
T * ℓ12	-1/ 36	-1/ 36	-1/ 100	-1/ 180	-1/ 72	1/ 600
T * ℓ21	-1/ 360	-1/ 360	-1/ 3600	1/ 360	-1/ 360	-1/ 900
T * ℓ22	-1/ 180	-1/ 72	1/ 600	1/ 180	-1/ 72	1/ 150
ℓ11**2	-1/ 200	-1/ 1260	1/ 600	-1/ 1050	-1/ 3150	0/ 1
ℓ12**2	-1/ 60	-1/ 60	-1/ 100	-1/ 315	-1/ 150	0/ 1
ℓ21**2	-1/ 4200	-1/ 4200	-1/ 3600	1/ 700	-1/ 3150	-1/ 1200
ℓ22**2	-1/ 1260	-1/ 200	1/ 600	1/ 210	-1/ 150	1/ 200
ℓ11 * ℓ12	-1/ 75	-2/ 315	0/ 1	-4/ 1575	-4/ 1575	0/ 1
ℓ11 * ℓ21	-1/ 525	-1/ 1575	0/ 1	-1/ 2100	-1/ 2100	-1/ 1800
ℓ11 * ℓ22	-4/ 1575	-4/ 1575	0/ 1	-1/ 1575	-1/ 525	0/ 1
ℓ12 * ℓ21	-4/ 1575	-4/ 1575	0/ 1	-1/ 1575	-1/ 525	0/ 1
ℓ12 * ℓ22	-2/ 315	-1/ 75	0/ 1	-1/ 630	-1/ 100	1/ 300
ℓ21 * ℓ22	-1/ 1575	-1/ 525	0/ 1	2/ 525	-4/ 1575	0/ 1

COEFFICIENTS OF L(I,J) FOR USE IN FORMING INITIAL STRAIN MATRIX

	(13,1)	(13,2)	(13,3)	(13,4)	(13,5)	(13,6)
L * T**2	3/ 20	3/ 20	1/ 4	-3/ 20	7/ 20	1/ 4
T * L11	-1/ 15	-1/ 15	-9/ 100	0/ 1	-1/ 12	-3/ 50
T * L12	-1/ 12	0/ 1	-3/ 50	0/ 1	0/ 1	-1/ 25
T * L21	0/ 1	-1/ 12	-3/ 50	1/ 15	-4/ 15	-9/ 100
T * L22	0/ 1	0/ 1	-1/ 25	1/ 12	0/ 1	-3/ 50
L11**2	-9/ 280	-9/ 280	-1/ 25	-1/ 280	-39/ 1400	-1/ 50
L12**2	-33/ 700	1/ 280	-1/ 50	-11/ 2100	13/ 4200	-1/ 100
L21**2	1/ 280	-33/ 700	-1/ 50	9/ 280	-27/ 140	-1/ 25
L22**2	11/ 2100	11/ 2100	-1/ 100	33/ 700	3/ 140	-1/ 50
L11 * L12	-39/ 700	-1/ 140	-1/ 25	-13/ 2100	-13/ 2100	-1/ 50
L11 * L21	-1/ 140	-39/ 700	-1/ 25	1/ 140	-33/ 350	-1/ 25
L11 * L22	-13/ 2100	-13/ 2100	-1/ 50	13/ 2100	-11/ 1050	-1/ 50
L12 * L21	-13/ 2100	-13/ 2100	-1/ 50	13/ 2100	-11/ 1050	-1/ 50
L12 * L22	-11/ 1050	13/ 2100	-1/ 50	11/ 1050	11/ 1050	-1/ 50
L21 * L22	13/ 2100	-11/ 1050	-1/ 50	39/ 700	-3/ 70	-1/ 25

	(13,7)	(13,8)	(13,9)	(13,10)	(13,11)	(13,12)
L * T**2	7/ 20	-3/ 20	1/ 4	-7/ 20	-7/ 20	1/ 4
T * L11	-1/ 12	0/ 1	-3/ 50	0/ 1	0/ 1	-1/ 25
T * L12	-4/ 15	1/ 15	-9/ 100	0/ 1	1/ 12	-3/ 50
T * L21	0/ 1	0/ 1	-1/ 25	1/ 12	0/ 1	-3/ 50
T * L22	0/ 1	1/ 12	-3/ 50	4/ 15	4/ 15	-9/ 100
L11**2	-39/ 1400	-1/ 280	-1/ 50	-13/ 4200	-13/ 4200	-1/ 100
L12**2	-27/ 140	9/ 280	-1/ 25	-3/ 140	39/ 1400	-1/ 50
L21**2	13/ 4200	-11/ 2100	-1/ 100	39/ 1400	-3/ 140	-1/ 50
L22**2	3/ 140	33/ 700	-1/ 50	27/ 140	27/ 140	-1/ 25
L11 * L12	-33/ 350	1/ 140	-1/ 25	-11/ 1050	13/ 2100	-1/ 50
L11 * L21	-13/ 2100	-13/ 2100	-1/ 50	13/ 2100	-11/ 1050	-1/ 50
L11 * L22	-11/ 1050	13/ 2100	-1/ 50	11/ 1050	11/ 1050	-1/ 50
L12 * L21	-11/ 1050	13/ 2100	-1/ 50	11/ 1050	11/ 1050	-1/ 50
L12 * L22	-3/ 70	39/ 700	-1/ 25	3/ 70	33/ 350	-1/ 25
L21 * L22	11/ 1050	11/ 1050	-1/ 50	33/ 350	3/ 70	-1/ 25

	(14,1)	(14,2)	(14,3)	(14,4)	(14,5)	(14,6)
L * T**2	0/ 1	-1/ 30	-1/ 24	3/ 20	-1/ 20	1/ 24
T * L11	1/ 90	1/ 60	1/ 50	-1/ 90	1/ 60	1/ 200
T * L12	1/ 72	0/ 1	1/ 75	-1/ 72	0/ 1	1/ 300
T * L21	-1/ 90	1/ 60	1/ 200	-1/ 18	1/ 30	-3/ 100
T * L22	-1/ 72	0/ 1	1/ 300	-5/ 72	0/ 1	-1/ 50
L11**2	1/ 140	3/ 350	1/ 100	-1/ 840	9/ 1400	1/ 300
L12**2	11/ 1050	-1/ 1050	1/ 200	-11/ 6300	-1/ 1400	1/ 600
L21**2	-1/ 210	3/ 350	0/ 1	-1/ 40	3/ 140	-1/ 50
L22**2	-11/ 1575	-1/ 1050	0/ 1	-11/ 300	-1/ 420	-1/ 100
L11 * L12	13/ 1050	1/ 525	1/ 100	-13/ 6300	1/ 700	1/ 300
L11 * L21	-1/ 420	9/ 700	1/ 150	-1/ 105	3/ 175	0/ 1
L11 * L22	-13/ 6300	1/ 700	1/ 300	-13/ 1575	1/ 525	0/ 1
L12 * L21	-13/ 6300	1/ 700	1/ 300	-13/ 1575	1/ 525	0/ 1
L12 * L22	-11/ 3150	-1/ 700	1/ 300	-22/ 1575	-1/ 525	0/ 1
L21 * L22	-13/ 1575	1/ 525	0/ 1	-13/ 300	1/ 210	-1/ 50

	(14,7)	(14,8)	(14,9)	(14,10)	(14,11)	(14,12)
L * T**2	0/ 1	1/ 30	-1/ 24	7/ 20	1/ 20	1/ 24
T * L11	1/ 72	0/ 1	1/ 75	-1/ 72	0/ 1	1/ 300
T * L12	2/ 45	-1/ 60	1/ 50	-2/ 45	-1/ 60	1/ 200
T * L21	-1/ 72	0/ 1	1/ 300	-5/ 72	0/ 1	-1/ 50
T * L22	-2/ 45	-1/ 60	1/ 200	-2/ 9	-1/ 30	-3/ 100
L11**2	13/ 2100	1/ 1050	1/ 200	-13/12600	1/ 1400	1/ 600
L12**2	3/ 70	-3/ 350	1/ 100	-1/ 140	-9/ 1400	1/ 300
L21**2	-13/ 3150	1/ 1050	0/ 1	-13/ 600	1/ 420	-1/ 100
L22**2	-1/ 35	-3/ 350	0/ 1	-3/ 20	-3/ 140	-1/ 50
L11 * L12	11/ 525	-1/ 525	1/ 100	-11/ 3150	-1/ 700	1/ 300
L11 * L21	-13/ 6300	1/ 700	1/ 300	-13/ 1575	1/ 525	0/ 1
L11 * L22	-11/ 3150	-1/ 700	1/ 300	-22/ 1575	-1/ 525	0/ 1
L12 * L21	-11/ 3150	-1/ 700	1/ 300	-22/ 1575	-1/ 525	0/ 1
L12 * L22	-1/ 70	-9/ 700	1/ 150	-2/ 35	-3/ 175	0/ 1
L21 * L22	-22/ 1575	-1/ 525	0/ 1	-11/ 150	-1/ 210	-1/ 50

COEFFICIENTS OF L(I,J) FOR USE IN FORMING INITIAL STRAIN MATRIX

	(15,1)	(15,2)	(15,3)	(15,4)	(15,5)	(15,6)
L * T**2	-1/ 30	0/ 1	-1/ 24	1/ 30	0/ 1	-1/ 24
T * L11	1/ 60	1/ 90	1/ 50	0/ 1	1/ 72	1/ 75
T * L12	1/ 60	-1/ 90	1/ 200	0/ 1	-1/ 72	1/ 300
T * L21	0/ 1	1/ 72	1/ 75	-1/ 60	2/ 45	1/ 50
T * L22	0/ 1	-1/ 72	1/ 300	-1/ 60	-2/ 45	1/ 200
L11**2	3/ 350	1/ 140	1/ 100	1/ 1050	13/ 2100	1/ 200
L12**2	3/ 350	-1/ 210	0/ 1	1/ 1050	-13/ 3150	0/ 1
L21**2	-1/ 1050	11/ 1050	1/ 200	-3/ 350	3/ 70	1/ 100
L22**2	-1/ 1050	-11/ 1575	0/ 1	-3/ 350	-1/ 35	0/ 1
L11 * L12	9/ 700	-1/ 420	1/ 150	1/ 700	-13/ 6300	1/ 300
L11 * L21	1/ 525	13/ 1050	1/ 100	-1/ 525	11/ 525	1/ 100
L11 * L22	1/ 700	-13/ 6300	1/ 300	-1/ 700	-11/ 3150	1/ 300
L12 * L21	1/ 700	-13/ 6300	1/ 300	-1/ 700	-11/ 3150	1/ 300
L12 * L22	1/ 525	-13/ 1575	0/ 1	-1/ 525	-22/ 1575	0/ 1
L21 * L22	-1/ 700	-11/ 3150	1/ 300	-9/ 700	-1/ 70	1/ 150

	(15,7)	(15,8)	(15,9)	(15,10)	(15,11)	(15,12)
L * T**2	-1/ 20	3/ 20	1/ 24	1/ 20	7/ 20	1/ 24
T * L11	1/ 60	-1/ 90	1/ 200	0/ 1	-1/ 72	1/ 300
T * L12	1/ 30	-1/ 18	-3/ 100	0/ 1	-5/ 72	-1/ 50
T * L21	0/ 1	-1/ 72	1/ 300	-1/ 60	-2/ 45	1/ 200
T * L22	0/ 1	-5/ 72	-1/ 50	-1/ 30	-2/ 9	-3/ 100
L11**2	9/ 1400	-1/ 840	1/ 300	1/ 1400	-13/12600	1/ 600
L12**2	3/ 140	-1/ 40	-1/ 50	1/ 420	-13/ 600	-1/ 100
L21**2	-1/ 1400	-11/ 6300	1/ 600	-9/ 1400	-1/ 140	1/ 300
L22**2	-1/ 420	-11/ 300	-1/ 100	-3/ 140	-3/ 20	-1/ 50
L11 * L12	3/ 175	-1/ 105	0/ 1	1/ 525	-13/ 1575	0/ 1
L11 * L21	1/ 700	-13/ 6300	1/ 300	-1/ 700	-11/ 3150	1/ 300
L11 * L22	1/ 525	-13/ 1575	0/ 1	-1/ 525	-22/ 1575	0/ 1
L12 * L21	1/ 525	-13/ 1575	0/ 1	-1/ 525	-22/ 1575	0/ 1
L12 * L22	1/ 210	-13/ 300	-1/ 50	-1/ 210	-11/ 150	-1/ 50
L21 * L22	-1/ 525	-22/ 1575	0/ 1	-3/ 175	-2/ 35	0/ 1

	(16,1)	(16,2)	(16,3)	(16,4)	(16,5)	(16,6)
L * T**2	0/ 1	0/ 1	1/ 144	-1/ 30	0/ 1	-1/ 144
T * L11	-1/ 360	-1/ 360	-1/ 225	1/ 360	-1/ 360	-1/ 900
T * L12	-1/ 360	1/ 360	-1/ 900	1/ 360	1/ 360	-1/ 3600
T * L21	1/ 360	-1/ 360	-1/ 900	1/ 72	-1/ 180	1/ 150
T * L22	1/ 360	1/ 360	-1/ 3600	1/ 72	1/ 180	1/ 600
L11**2	-1/ 525	-1/ 525	-1/ 400	1/ 3150	-1/ 700	-1/ 1200
L12**2	-1/ 525	2/ 1575	0/ 1	1/ 3150	1/ 1050	0/ 1
L21**2	2/ 1575	-1/ 525	0/ 1	1/ 150	-1/ 210	1/ 200
L22**2	2/ 1575	2/ 1575	0/ 1	1/ 150	1/ 315	0/ 1
L11 * L12	-1/ 350	1/ 1575	-1/ 600	1/ 2100	1/ 2100	0/ 1
L11 * L21	1/ 1575	-1/ 350	-1/ 600	4/ 1575	-2/ 525	0/ 1
L11 * L22	1/ 2100	1/ 2100	-1/ 1800	1/ 525	1/ 1575	0/ 1
L12 * L21	1/ 2100	1/ 2100	-1/ 1800	1/ 525	1/ 1575	0/ 1
L12 * L22	1/ 1575	1/ 525	0/ 1	4/ 1575	4/ 1575	0/ 1
L21 * L22	1/ 525	1/ 1575	0/ 1	1/ 100	1/ 630	1/ 300

	(16,7)	(16,8)	(16,9)	(16,10)	(16,11)	(16,12)
L * T**2	0/ 1	-1/ 30	-1/ 144	-1/ 20	-1/ 20	1/ 144
T * L11	-1/ 360	1/ 360	-1/ 900	1/ 360	1/ 360	-1/ 3600
T * L12	-1/ 180	1/ 72	1/ 150	1/ 180	1/ 72	1/ 600
T * L21	1/ 360	1/ 360	-1/ 3600	1/ 72	1/ 180	1/ 600
T * L22	1/ 180	1/ 72	1/ 600	1/ 36	1/ 36	-1/ 100
L11**2	-1/ 700	1/ 3150	-1/ 1200	1/ 4200	1/ 4200	-1/ 3600
L12**2	-1/ 210	1/ 150	1/ 200	1/ 1260	1/ 200	1/ 600
L21**2	1/ 1050	1/ 3150	0/ 1	1/ 200	1/ 1260	1/ 600
L22**2	1/ 315	1/ 150	0/ 1	1/ 60	1/ 60	-1/ 100
L11 * L12	-2/ 525	4/ 1575	0/ 1	1/ 1575	1/ 525	0/ 1
L11 * L21	1/ 2100	1/ 2100	-1/ 1800	1/ 525	1/ 1575	0/ 1
L11 * L22	1/ 1575	1/ 525	0/ 1	4/ 1575	4/ 1575	0/ 1
L12 * L21	1/ 1575	1/ 525	0/ 1	4/ 1575	4/ 1575	0/ 1
L12 * L22	1/ 630	1/ 100	1/ 300	2/ 315	1/ 75	0/ 1
L21 * L22	4/ 1575	4/ 1575	0/ 1	1/ 75	2/ 315	0/ 1